sSl. No.	IIT Ropar List of Recent Publications with Abstract Coverage: May, 2026
A	**Book Chapter(s)**
1.	Classification of gamma radiation: Insights into terrestrial and cosmic sources **SS Kaintura,** M Prasad, T Sharma, **PP Singh** - Natural Gamma Radiation: Sources, Devices and Measurement, Detection Usefulness, and Hazards: Book Chapter, 2026 **Abstract:** Radiation from natural sources is an inescapable and pervasive aspect of existence on the planet Earth. Approximately 80% of the total radiation stems from natural radioactivity in the ambient radiation background of Earth's Environment. Natural radioactivity can be bifurcated further, for which, terrestrial and cosmogenic radionuclides are responsible. Terrestrial environments consist of naturally occurring radioactive materials (NORMs), constituting the primary source of radiation exposure for humans. Primordial radionuclides, such as ^{238}U, ^{232}Th, ^{40}K, and ^{235}U, originate from nucleosynthesis processes in stars, boasting extraordinarily long half-lives. The susceptibility of living organisms to radiation depends on the naturally occurring gamma-emitting radionuclides in the rock and soil of a specific geographic area. High-energy subatomic particles from space, known as cosmic radiation, continuously bombard Earth's surface. These particles interact with atmospheric nuclei, producing cosmogenic radionuclides (^{3}He, ^{7}Be, ^{14}C, and ^{22}Na) and secondary reaction products. Exposure to cosmic rays increases with higher altitudes. This chapter presents a comprehensive overview of the classification of gamma radiation, with a special focus on terrestrial and cosmic radiations. Efforts are made to shed light on diverse origins, properties, and implications for both terrestrial and cosmic radiations. The information presented in this chapter will be useful in advancing scientific knowledge, ensuring radiation safety, and facilitating technological developments in diverse fields.
2.	Clean air insights evaluating the impact of pollution control regulations in India **S Dey** - Harnessing Computational Power to Tackle Air Pollution: Book Chapter, 2026 **Abstract:** As air pollution continues to pose significant health and environmental challenges in India, the effectiveness of pollution control regulations has become a focal point for policymakers and researchers. Therefore, this study presents Clean Air Insights to assess the impacts of air pollution control regulations in various regions of India. The proposed framework uses advanced analytical techniques using a large dataset that combines historical air quality measurements, regulatory timelines, and socioeconomic indicators to evaluate the effectiveness of implemented policies. This study analyzes the relationships between regulatory interventions and changes in air quality using the designed *Average Treatment Effect* metric. The prediction accuracy is computed using the designed *custom accuracy* metric. Experimental results reveal significant correlations between stringent pollution control measures and air quality improvements, highlighting the effectiveness of specific regulations in mitigating emissions approximately 60% from Bayesian LSTM model. Additionally, this analysis uncovers regional disparities in response to these regulations, providing valuable information for targeted policy adjustments.
3.	Enhancing industrial emission predictions with the AirGuard framework **S Dey** - Harnessing Computational Power to Tackle Air Pollution: Book Chapter, 2026 **Abstract:** Industrial activity grows, so do environmental concerns, making it essential to keep track of air pollution for sustainable progress. Therefore, this work introduces a novel machine learning-based framework: AirGuard, to predict and analyze factory emissions. The proposed framework designs synthetic data and proceeds with the proposed *Heuristic Bidirectional Gated*

	Recurrent Neural Network (HoG) model to predict air quality levels in industrial areas. Additionally, AirGuard employs time series forecasting and heuristic-based regression analysis to identify industrial emission rates and their temporal variations as the heuristic-based HoG model efficiently understands past emission patterns and identifies influencing factors. These analyses help improve prediction accuracy and support proactive emission control strategies. The experimental results described that the AirGuard framework improves the accuracy of industrial pollution predictions and provides helpful information on emission patterns. Using AirGuard helps industries comply with regulations and take proactive steps to reduce pollution, making AirGuard a valuable tool for environmental management and promoting more innovative and sustainable industrial practices.
4.	Ionic liquid nanoparticles in biomass processing **S Jaswal, A Sharma, SS Bhalri**, N Kaur, **N Singh** - Ionic Liquids in Biomass Processing: Green Protocols: Book Chapter, 2026 **Abstract:** Research on biomass as a potential feedstock for biofuels, chemicals, and advanced materials has increased significantly due to the growing need for sustainable raw materials and renewable energy worldwide. Lignocellulosic biomass, a renewable substitute for fossil fuels, due to its structural complexity, possesses resistance to efficient and economical production of biochemicals. Ionic liquid nanoparticles (IL-NPs), in particular, have demonstrated significant promise in recent nanotechnology breakthroughs for tackling these issues. The function of nanomaterials based on Fe_3O_4, SiO_2, ZnO, etc., was used with ionic liquids (ILs) in the biomass processing, and their applicabilities are the main topic of this chapter, with a particular emphasis on how they support sustainable and environmentally friendly practices. We have classified discussions on biodiesel, bioethanol, and miscellaneous valuable biogenic end products. Special attention is given to energy savings, recyclability of ILs, and the reduction of harmful byproducts.
5.	Materials for 3D printing in medicine **A Sarkar, B Das** - Healing in Layers: 3D Printing in Healthcare: Book Chapter, 2026 **Abstract:** Almost over the past four decades, 3D printing has been gaining much interest as an assembly procedure because of its nonexclusive and layer-by-layer construction method involving zero wastage of raw material with accurate precision even for smaller architectures. Later on, by incorporating standard biocompatible materials in the printing machinery even with actual cells, different cellular growth factors, and bioactive compounds like proteins, the same method progressed into 3D bioprinting for tissue buildings, making its way into medicine. This can construct orthopedic bioactive implants with appropriate architecture for bone or organ support, medical devices, tissue engineering scaffolds, ideal tissues and organs for organ transplantation, drug screening, disease modeling, and so on. Depending on the type of biomaterial employed and how the layers need to be connected to the component, different techniques like fused deposition modeling, extrusion-based bioprinting, selective laser sintering, etc. come into functioning. Biocompatibility comes as the first criterion for choosing any biomaterial intended for application in medicine. Bioink constituting cells and one or multiple biomaterials along with different growth factors leads to the printing of cell-laden structures like organs. These can also generate illness and organ failures due to biomaterial-related infections. Thus, natural biomaterials, surface-treated biomaterials, etc., have been employed for the biofabrication of 3D-printed structures rendering no biological rejection. This chapter covers a comprehensive evaluation of different materials used in 3D printing and 3D bioprinting for medicinal purposes which include metals, polymers, ceramics, composites, and bioinks, and their recent and ongoing innovations and adaptations in the development of human care products in the field of medicine. Significant advantages of this method like the capability of producing complex geometries with utmost precision, relatively shorter fabrication periods, low

	manufacturing costs, and ability to produce controllable structures have paved its way through research academics, industry, and so on.
B	**Conference Proceeding(s)**
6.	A case study for designing digital assistance systems for smart factories with eye-tracking support **J Singh,** S Gupta - Biennial International Conference on Future Learning Aspects of Mechanical Engineering (FLAME 2024), 2026 **Abstract:** Cognitive aid systems can provide the greatest degree of flexibility and personalization while allowing users to obtain useful assistance with their industrial work duties. Eye-tracking technology as a fundamental element of cognitive aid systems to maximize worker performance in human–cyber–physical systems is investigated in this study. Real-time visual attention analysis is made possible by eye tracking, which offers valuable information on task engagement, skill levels, and cognitive load during intricate manual tasks. The use of these technologies is illustrated by a case study involving the electronic car battery module housing quality measurement. The findings, which were confirmed by ANOVA analysis, show that fixation times vary significantly among skill levels with experts exhibiting noticeably faster reactions. These results highlight how important it is to include eye-tracking data into context-sensitive, adaptive cognitive support systems that improve worker productivity and decision-making. This study demonstrates how visual attention measures may be utilized to develop more intelligent, user-focused solutions for Industry 4.0 applications.
7.	ANN based early insulation degradation index (EIDI) for predictive maintenance of XLPE power cables N Rishik…**CC Reddy** - Third International Conference on Networking and Communications (ICNWC), 2026 **Abstract:** Monitoring the state of healthy XLPE high voltage cables is of paramount importance in case you do not want to incur expensive outage costs. Many of the standard inspections, such as inspecting tan delta, inspecting partial discharges, or inspecting a withstand voltage test, are reactive; they spot problems only after the insulation is already defective. In this paper, therefore, we proposed a new, non invasive early trouble identification method, based on an Artificial Neural Network, which computes a score, which we call the Early Insulation Degradation Index (EIDI). The point is to test the harmonic distortion, leakage current, and temperature changes of the cable when it is running under normal conditions, and based on this data to determine whether the insulation is beginning to creep. We also trained the ANN using both simulated data and real world measurements to ensure that the ANN learns the correlation between electrical stresses and ageing to provide me with an EIDI score ranging between 0 and 1. We also established the limits at 0.3, 0.6 and 0.85 to declare the insulation as healthy, moderate or critical to make the maintenance go before the problems become sever. The experiments demonstrate that the model is capable of hitting approximately 94.1% accuracy and it can foretell breakdowns weeks before they happen. It implies that we are replacing the old and off the shelf diagnostics with the continuous, data driven one that can actually be used to monitor underground and submarine high voltage cables.
8.	Assessing applicability and adoption of agriculture-centric computation technologies in Punjab: A multi-district farmer survey M Zala, S Gupta, **SS Kaintura, PP Singh,** N Kaur - International Conference on Agriculture-Centric Computation (ICA 2025), 2026

	Abstract: The state of Punjab played a crucial role in turning India into a surplus food producer in the 1970s and was celebrated as the "wheat basket" during the Green Revolution. However, the last three decades have revealed the aftermath of imprudent use of technology interventions, leading to severe social, economic, and environmental degradation. This study examines current farming practices across 200 villages by surveying 600 farmers in the state. It assesses farmers' education, gender, farming experience, landholding, agrochemical use, irrigation practices, climate change impact and awareness on new agriculture policies and advancements. The findings reveal gender disparity, low education levels, youth disinterest in farming, and predominantly small to medium landholders. Additionally, excessive agrochemical use, monocropping, and over-extraction of groundwater are major sustainability concerns, exacerbated by unpredictable weather patterns resulting from climate change. The research identifies critical knowledge, and technology gaps and highlights how these can be addressed through agriculture-centric computation solutions. Given their interdisciplinary nature, effective interventions demand a collaborative approach that integrates human expertise with agriculture-centric computation technologies including precision agriculture (PA), AI/ML models, IoT, and data-driven decision-making to bridge these gaps, and drive a transition in Punjab's agricultural ecosystem.
9.	Assessment of osteonecrosis-induced changes in the viscoelastic and biomechanical properties of human trabecular bone RK Bhushan, AM Kurup, **N Kumar,** N Kumar - IEEE International Biomedical Instrumentation and Technology Conference (IBITeC), 2026 **Abstract:** Osteonecrosis is a degenerative condition that disrupts bone's structural integrity and raises the likelihood of fragility-related fractures. Because bone is viscoelastic, its mechanical performance varies with the applied loading rate. This investigation examines how osteonecrosis influences the viscoelastic response of human trabecular bone and explores its relationship to microstructural and mechanical features. Trabecular bone samples were collected from femoral heads of 18 patients with osteonecrosis, all with hip fragility fractures. From each femur head, both the necrotic and healthy regions were sampled for analysis. Micro-computed tomography (micro-CT) was used to assess bone architecture. Dynamic mechanical analysis (DMA) and Stress relaxation tests were conducted to characterize viscoelastic behavior. Statistical correlation was applied to determine links between viscoelasticity, microstructural indices, and biomechanical parameters. Osteo-necrotic bone exhibited markedly different stress relaxation and frequency sweep profiles compared to healthy bone. Reduced storage modulus, initial stress, and initial stiffness were evident in the diseased group. Stress relaxation percentage correlated inversely with mineral content ($r = -0.52$, $p = 0.003$) and mineral-to-matrix ratio ($r = -0.43$, $p = 0.009$), and directly with organic content ($r = 0.40$, $p = 0.02$). Storage and loss modulus values also showed significant associations with volume fraction of bone (BV/TV) across both regions. The findings indicate that osteonecrosis alters the time-dependent mechanical performance of trabecular bone (femoral). Higher organic content appears beneficial for viscoelastic function, whereas excessive mineralization reduces it. These results highlight the role of compositional changes in weakening osteonecrotic bone and increasing fracture susceptibility.
10.	BreathSense: Breathing rate estimation from microphone-acquired audio using adaptive filtering and machine learning framework **A Hari, VK Maurya, P Srivastava, A Chanda, B Kumbhani** - IEEE International Symposium on Smart Electronic Systems (iSES), 2026 **Abstract:** Respiratory rate (RR) is a critical biomarker for assessing physiological and clinical health, with continuous monitoring offering valuable insights into early signs of respiratory and systemic disorders. Despite its importance, accurate RR estimation from audio signals remains a

	challenging task due to ambient noise, dynamic acoustic environments, and low signal-to-noise ratios. This study presents a robust, audio-based respiratory monitoring framework designed to address these challenges through the integration of adaptive signal processing and machine learning techniques. Respiratory sounds are acquired using a microphone and processed via an Adaptive Line Enhancer (ALE) employing the Normalized Least Mean Square (NLMS) algorithm. This adaptive filter dynamically attenuates non-stationary noise while preserving the periodic components associated with breathing. The resulting denoised signal is analyzed in the frequency domain using the Fast Fourier Transform (FFT) to identify dominant respiratory frequencies. Furthermore, a regression-based machine learning model is trained on a combination of time- and frequency-domain features to enhance the accuracy and generalizability of RR estimation under diverse acoustic conditions. The proposed system provides a non-invasive, real-time, and scalable solution for continuous respiratory monitoring in clinical, wearable, and remote healthcare settings.
11.	Determination of energy absorption capacity of NRL and SBR across rock joints **K Saha, R Sebastian** - 13th Asian Rock Mechanics Symposium (ARMS 2024), 2026 **Abstract:** Shear waves can be propagated through jointed rocks due to various sources such as earthquakes, mining, and blasting. This research uses the Split Shear Plate (SSP) facility for generating shear waves in rock plates in the laboratory. The SSP apparatus is commonly used for investigating the dynamic properties of materials during wave propagation. The SSP consists of a friction bar, a supporting block, incident and transmitted plates, separated by a joint. Shear wave propagation across jointed rocks with rubber infill materials was studied. Piezoelectric accelerometers were used at different locations within filled rock joints to record the vibrations. Commercially produced synthetic rubber, Styrene Butadiene Rubber (SBR) latex, and naturally abundant available Natural Rubber (NR) latex were chosen as infill materials. Recorded acceleration-time (a–t) histories were used to determine the energy absorption capacity of NR latex and SBR latex across rock joints. SBR latex was found to be more effective in shock absorption than NR latex.
12.	Determination of fragment ejection velocity of rock fragment under uniaxial compression loading before rock-burst using infrared thermography **M Jaiswal, R Sebastian,** R Mulaveesala - 13th Asian Rock Mechanics Symposium (ARMS 2024), 2026 **Abstract:** The infrared thermography technique was employed to analyze the ejection velocity characteristics of rock fragments in uniaxial compression testing. The velocity components of the fragments were found to be correlated with the infrared radiation characteristics of the rock sample during the loading process. The estimation of the initial fragment ejection velocity prior to the burst can be achieved by analyzing the peak temperature deviation and infrared radiation characteristics. Moreover, the assessment of the kinetic energy of fragments involved the consideration of both the initial ejection velocity and the mass of the pieces within each size group. The findings indicate that the velocity of a fragment is contingent upon the specific rock type and brittleness of the rock. The acceleration of the fragment movement in a rock is attributed to the propagation of stress waves and the opening of cracks, both of which contribute to the fluctuations in peak and average temperatures. Kinetic energy constitutes a fraction of the overall dissipated energy during a burst, and this fraction is directly linked to the average infrared temperature differential of the rock.
13.	Effective and robust multimodal medical image analysis **J Dhar,** N Zaidi, M Haghighat - 32nd ACM SIGKDD Conference on Knowledge Discovery and Data Mining V.1, 2026

	Abstract: Multimodal **F**usion **L**earning (MFL), leveraging disparate data from various imaging modalities (e.g., MRI, CT, SPECT), has shown great potential for addressing medical problems such as skin cancer and brain tumor prediction. However, existing MFL methods face three key limitations: a) they often specialize in specific modalities, and overlooks effective shared complementary information across diverse modalities, hence limiting their generalizability for multi-disease analysis; b) they rely on computationally expensive models, restricting their applicability in resource-limited settings; and c) they lack robustness against adversarial attacks, compromising reliability in medical AI applications. To address these limitations, we propose a novel **M**ulti-**A**ttention **I**ntegration **L**earning (MAIL) network, incorporating two key components: a) an efficient residual learning attention block for capturing refined modality-specific multi-scale patterns and b) an efficient multimodal cross-attention module for learning enriched complementary shared representations across diverse modalities. Furthermore, to ensure adversarial robustness, we extend MAIL network to design Robust-MAIL by incorporating random projection filters and modulated attention noise. Extensive evaluations on 20 public datasets show that both MAIL and Robust-MAIL outperform existing methods, achieving performance gains of up to 9.34% while reducing computational costs by up to 78.3%. These results highlight the superiority of our approaches, ensuring more reliable predictions than top competitors.
14.	Exploring dynamic properties of frictional jointed rocks: The impact of joint roughness **S Rohilla, R Sebastian** – 13th Asian Rock Mechanics Symposium (ARMS 2024), 2026 **Abstract:** Evaluating dynamic properties in rocks is critical in addressing various challenges within rock engineering. The mechanical behaviour of rocks exhibits variations under static, cyclic, and dynamic loading conditions. This research investigates the influence of joint roughness on the dynamic properties of frictional jointed rocks, specifically those with matched single joints. Gypsum plaster was utilised to fabricate frictional jointed rock specimens with artificially introduced joint roughness coefficients (JRC) of 6–8, 12–14, and 18–20. Cyclic torsional shear tests were performed on these single-jointed rocks, exploring a range of experimental conditions, including strain amplitude, frequency, confining pressure, and the number of cycles. The study aims to elucidate the individual and combined effects of these parameters on the shear modulus and damping ratio of frictional jointed rocks across varying JRCs. The research identifies the variation in shear modulus and damping ratio of single-jointed rocks concerning individual joint characteristics (i.e., JRC) and loading characteristics (i.e., frequency, confining pressure, strain amplitude, and number of cycles). The study analyses the combined influence of material properties and loading characteristics on the dynamic properties of frictional jointed rocks through regression analysis. This research holds potential applications in scenarios where rock masses undergo repetitive cyclic loading.
15.	LeADS (leaf anomaly detection system): Deep learning pipeline for leaf stress, disease & severity estimation **MP Das, N Goel, M Saini** - International Conference on Agriculture-Centric Computation (ICA 2025), 2026 **Abstract:** Leaves are amongst the most sensitive parts of a plant. Any anomaly in the plant often affects the leaves first. Understanding the exact cause of leaf anomaly is a multi-faced challenge. We have come up with a novel end-to-end leaf anomaly detection system that differentiates between stressed and diseased leaf in the first stage using custom InceptionV3 model. Then it detects the exact type of disease and localizes the affected leaf area in the second stage using two YOLOv8 models. At last, it estimates the severity of the detected disease in the third stage using YOLO detections and IoU calculations. We have used Transfer Learning to use pre-trained

	weights. Our system is able to detect multiple anomalies on a single image. Classification task has 92% accuracy while Object Detection task and Severity estimation has about 80% accuracy.
16.	Navigating financial instability: An interpretable paradigm for multi-label crisis prediction R Kaur, **G Singh,** D Guha - IEEE Afro-Mediterranean Conference on Artificial Intelligence (AMCAI), 2026 **Abstract:** We present a rigorous methodology for applying Elastic Weight Consolidation (EWC) to the continual prediction of banking, systemic, currency and inflation crises. Traditional models, trained on earlier regimes, are prone to catastrophic forgetting when updated on new regimes for financial crisis prediction that is a sequential, non-stationary learning problem with data arriving across time and heterogeneous jurisdictions. EWC mitigates this by constraining important parameters, quantified via a diagonal-Fisher-information approximation, to remain near previously learnt optima while permitting flexibility in less critical directions. We formalise the Bayesian derivation underpinning EWC, present the practical diagonalFisher estimator, and integrate the method into a reproducible training pipeline for multi-label crisis prediction. Our protocol uses representative task partitions, rigorous Fisher estimation, lambda scheduling, and a suite of evaluation metrics to compare performance with baseline traditional models. We provide ablation studies for Fisher estimation, penalty aggregation, and sequential walk-forward evaluation, and discuss limitations and interpretability for policy use. Our experimental model is tested for 2 years prior financial crisis prediction on Harvard Business School's global crisis database for 42 years and 70 countries, and it demonstrates ROC-AUC of in inflation crises, in systemic crises, 77.63% in currency crises and 67.51% in banking crises predictions, outperforming the traditional models' results. We also assess the sensitivity of EWC to its core hyperparameters for real-world application. By integrating SHAP, this work aims to bridge probabilistic continual-learning theory and operational early-warning systems, making models both interpretable and robust in dynamic financial environments.
17.	Personalized stress detection through reinforcement learning based domain adaptation **S Kochhar, N Thakur**…**DR Bhatula** - IEEE 23rd International Symposium on Biomedical Imaging (ISBI), 2026 **Abstract:** Personalized stress detection aims to model individual-specific physiological and behavioral patterns; however, such personalization requires effective knowledge transfer across users, particularly in data-scarce healthcare settings. A key challenge lies in identifying the most relevant source data for a new target user, as transferring knowledge from all sources can introduce negative transfer and degrade performance. To address this, we introduce Target-Aware Reward-Optimized Selection (TAROS), a reinforcement learning based framework that adaptively selects source samples most relevant to the target domain. The Deep Q-Network (DQN) agent learns optimal selection policies by approximating Q-values, ensuring that only informative and contextually aligned samples contribute to the adaptation process. We evaluate TAROS on a real-world, multi-user stress detection dataset characterized by high inter-subject variability. Experimental results show substantial improvements across multiple evaluation metrics compared to conventional methods, demonstrating that TAROS effectively mitigates negative transfer and significantly enhances personalized inter-subject adaptation.
18.	Recent developments in RFID reader antennas: A survey **R Raina, A Sharma** - IEEE International Symposium on Smart Electronic Systems (iSES), 2026 **Abstract:** The Internet of Things (IoT) concept strives to enhance intelligence in systems by minimizing human involvement and enabling automated communication. In this context, radio frequency identification (RFID) readers play a vital role in identifying objects and transmitting data within an IoT network. The efficiency of these readers largely depends on the performance

	of their built-in or externally connected antennas. This article presents a comprehensive review of advanced RFID reader antenna designs and the key challenges associated with them. The antennas are evaluated based on parameters such as operating frequency bands, gain and the polarisation. Various technical issues such as limited bandwidth, bidirectional radiation patterns, low gain, linear polarisation and large physical size are explored. Since low antenna gain negatively affects the reader's detection range, enhancing gain is a critical component. One effective approach involves integrating an artificial magnetic conductor (AMC) beneath the antenna. This setup suppresses backward radiation, thereby improving peak gain and promoting unidirectional radiation patterns.
19.	Uplink rate splitting multiple access based multi-AUV data transmission strategy for advanced underwater acoustic communication **S Kumar, S Bhattacharyya, S Darshi,** A Bansal, AA Jacob - 10th International Conference on Computer and Communication Engineering (ICCCE), 2026 **Abstract:** This paper explores the application of uplink rate splitting multiple access (RSMA) in underwater acoustic communication. With the increase in underwater nodes, existing multiple access techniques may be insufficient to meet quality-of-service (QoS) for advanced underwater applications. This challenge may be addressed by incorporating next-generation multiple access technologies, which offer higher data rates and throughput. Recently, RSMA has emerged as a new multiple access technique that provides a higher data rate and improved interference management than other prevalent methods. This work proposes the deployment of uplink RSMA in underwater acoustic communication, allowing m-AUVs to transmit data simultaneously while efficiently managing the detrimental effects of interference. A generalized framework for uplink communication is developed, and the impact of the dynamic underwater environment on the system performance is discussed. Performance evaluation metrics, such as rate, throughput, and outage, are used to demonstrate the effectiveness of RSMA in underwater acoustic communication compared to prevalent techniques.
C	**Article(s)**
20.	2-Local derivations on symmetrizable kac-moody lie algebras N Nehra, **S Rani** - Algebra Colloquium, 2026 **Abstract:** We establish that every 2-local inner derivation on a symmetrizable Kac-Moody Lie algebra g(A) over the field C is a derivation. In addition, we demonstrate that if dim(g(A)/g(A)′)≥2, where g(A)′=[g(A),g(A)] is the derived subalgebra of g(A), then g(A) admits a 2-local derivation which is not a derivation.
21.	A machine learning framework for DDoS attack detection in SDN-enabled mobile wireless networks **I Sharma, S Agarwal, SS Jha,** S Chakravarty - IEEE Access, 2026 **Abstract:** Attacks on network components and devices pose a significant threat to service continuity, necessitating robust detection mechanisms. This paper presents a Distributed Denial of Service (DDoS) attack detection framework tailored for heterogeneous mobile wireless networks within a Software-Defined Networking architecture. A two-tier model is proposed: localized attack detection at access points (APs) using a Multi-Layer Perceptron (MLP) classifier, and centralized detection under mobility at the controller using a Long Short-Term Memory (LSTM) model. The system incorporates novel traffic features such as flow count, speed of source IP, source and destination IP address entropy, proportion of bidirectional flows, and handover frequency, which together enhance detection in mobile environments. An LSTM model analyzes inter-AP traffic correlation over time to address mobility-driven DDoS attack

	amplification. The proposed approach is evaluated under diverse traffic types (TCP, UDP, ICMP) and varying attack intensities. The MLP model selected for integration into the framework demonstrates consistently strong detection capability across the evaluated scenarios, achieving accuracy values in the range of 95%–99% and showing improved performance relative to existing state-of-the-art schemes. Furthermore, multi-run statistical validation confirms stable behavior under randomized initialization and mobility-driven conditions, while controller-level correlation analysis enhances robustness against mobility-driven attack propagation.
22.	A multi-stage detection framework for wideband spectrum sensing **A Ahmad, K Kumar, S Agarwal,** S Chakravarty - IEEE Open Journal of the Communications Society, 2026 **Abstract:** We present WISDOM, a hardware-aware, blind wideband spectrum-sensing framework designed to bridge the gap between theoretical detection algorithms and the reality of low-cost radio front-ends. Unlike conventional detectors that suffer from the SNR wall, WISDOM operates entirely in the digital domain using a multi-stage statistical pipeline. The framework introduces three core novelties: (i) a Noise-Avoidance Criterion (η_n) derived via Ordered-Statistic Constant False Alarm Rate on a guaranteed noise-only spectral region manufactured by the pre-processing chain; (ii) an inverted *"Count-and-Slope"* decision rule that identifies signals by detecting structured local spectral deviations rather than absolute power thresholds; and (iii) an analytically scalable Selective Spectral Refinement. Extensive validation on Software Defined Radio testbeds demonstrates sensitivity of -85 dBm across a 50 MHz sensing bandwidth and acceptable performance against hardware impairments.
23.	A note on Wilf's conjecture **T Chatterjee, P Narula** - Semigroup Forum, 2026 **Abstract:** Wilf's conjecture gives the relationship between the embedding dimension, the Frobenius number, and the genus of a numerical semigroup. Consider a numerical semigroup S = a1, a2,..., ad minimally generated by d coprime positive integers, where a1 denotes the multiplicity of S. In 2015, Moscariello and Sammartano [9] established the validity of Wilf's inequality for all those numerical semigroups where a1 is sufficiently large and all the prime divisors of a1 are greater than or equal to ρ, for every fixed value of ρ= a1 d. In this article, we relax the arithmetic constraint on the prime divisors of a1 by replacing it with the more natural condition gcd(a1, a2) = 1, thereby significantly enlarging the family of numerical semigroups known to satisfy Wilf's Conjecture. Moreover, under this hypothesis, we sharpen the bound on a1 appearing in the work of Moscariello and Sammartano. As a consequence, our results not only extend their theorem to a wider class of numerical semigroups but also demonstrate that Wilf's inequality holds under strictly improved numerical bounds.
24.	A parallelizable algorithm for constrained maximization of preferences in large time-dependent graphs **KK Dutta,** V Gunturi - GeoInformatica, 2026 **Abstract:** The growing availability of large-scale transportation data has transformed urban mobility by enabling a wide range of preferences in route choices. One such problem is the maximization of a preference metric (e.g., safety, ease of navigation, or scenic appeal) while adhering to certain upper bound on travel-time. Such route planning problems have diverse use-cases in urban navigation. However, determining routes which maximize a preference metric, while adhering to an upper bound on travel-time, is computationally hard. This problem can be reduced to an instance of the Arc Orienteering Problem (AOP) which is known to be an NP-Hard problem. Although there have been works which attempted to develop heuristics for this problem, they are limited in their solution quality due their myopic search strategy. Moreover, their

	inherent serial nature limits their ability to harness the benefits of increasingly available parallel processing offered by modern multi-core processors. This shortcoming of the current state of the art severely limits their use in large-scale deployments. To address these limitations, this paper proposes a novel recursive algorithm that explores the solution space more comprehensively while intelligently reusing the intermediate results (across recursive calls) to improve performance. Furthermore, the algorithm's computational structure is inherently parallelizable, enabling it to fully exploit modern multi-core architectures through existing scheduling frameworks. Extensive experiments on large, real-world road networks demonstrate that this approach yields, on average, 1.29x improvement over the state of the art in terms solution quality, while maintaining (or better in some case) comparable runtime. Lastly, our algorithm exhibits near-linear speedup as the number of processing cores increases, underscoring both its scalability and practical applicability.
25.	A resilience framework for bi-criteria combinatorial optimization with bandit feedback V Aggarwal, **S Jain, S Pokhriyal,** CJ Quinn - Transactions on Machine Learning Research, 2026 **Abstract:** We study bi-criteria combinatorial optimization under noisy function evaluations. While resilience and black-box offline-to-online reductions have been studied in single-objective settings, extending these ideas to bi-criteria problems introduces new challenges due to the coupled degradation of approximation guarantees for objectives and constraints. We introduce a notion of (α, β, δ, N)-resilience for bi-criteria approximation algorithms, capturing how joint approximation guarantees degrade under bounded (possibly worst-case) oracle noise, and develop a general black-box framework that converts any resilient offline algorithm into an online algorithm for bi-criteria combinatorial multi-armed bandits with bandit feedback. The resulting online guarantees achieve sublinear regret and cumulative constraint violation of order$\tilde{O}(\delta^{2/3}N^{1/3}T^{2/3})$ without requiring structural assumptions such as linearity, submodularity, or semi-bandit feedback on the noisy functions. We demonstrate the applicability of the framework by establishing resilience for several classical greedy algorithms in submodular optimization.
26.	Assessing the influence of Köppen–Geiger climatic zones on ungauged prediction of design floods within rivers of peninsular India **AK Singh, SR Chavan** - ISH Journal of Hydraulic Engineering, 2026 **Abstract:** Accurate flood quantile estimation at ungauged sites is essential in water resource planning and flood risk management. Regional Flood Frequency Analysis (RFFA) based on the L-moment framework offers a robust and computationally efficient approach for estimating flood quantiles, particularly in data-scarce or ungauged catchments. Recent studies highlight the advantages of LH moments (i.e. higher-order probability-weighted moments), which provide enhanced sensitivity to distributional tails and improve the representation of extreme flood events. This paper assesses the influence of Köppen–Geiger climatic zones (i.e. arid, temperate, and tropical) on design flood estimation for ungauged rivers of peninsular India. The Conventional Index Flood method is compared with a recently proposed RFFA approach tailored for general peak discharge distribution datasets within the LH-moment framework, treating climatic zones as homogeneous regions. Results indicate higher heterogeneity in the arid zone, while the tropical zone is relatively homogeneous. Regional goodness-of-fit tests identify the GEV and GLO distributions as suitable regional distributions for the arid region, whereas the GLO distribution is more appropriate for the tropical region. The findings support improved flood risk assessment and infrastructure design and contribute to the development of more reliable, climate-sensitive flood management strategies.
27.	Assessing the short, medium, and long-term impacts of climate change on crop water availability of maize and paddy. **A Bashir, I Sonkar, SR Chavan** - Journal of Earth System Science, 2026

	Abstract: Sustainable water resource planning necessitates understanding the impacts of climate change on agriculture. This study investigates water availability for paddy (*Oryza sativa*) and maize (*Zea mays*) under climate change in the upper Indo-Gangetic floodplain of India. Future monthly projections of climate variables are downscaled using SVR and disaggregated to daily inputs for a root water uptake (RWU) model. The RWU model simulates irrigation water requirement (IWR) and relative crop yield (Y_r) using root-zone soil moisture dynamics. The study utilizes coupled model intercomparison project phase 6 (CMIP-6) projections from four general circulation models (GCMs) and five shared socioeconomic pathways (SSPs) to project IWR and Y_r for near (2015–2043), mid (2044–2071), and far (2072–2099) futures. For paddy, potential evapotranspiration (PET) trends are insignificant and mean seasonal rainfall (MSR) has Sen's slope of 0.54, 2.11 (99% confidence), and 2.42 (99% confidence) for the near, mid, and far future, respectively. The same is observed in the case of maize, for which Sen's slope of MSR in SSP5-8.5 for near, mid, and far time periods are 0.44, 1.94, and 2.00 within 95%, 99%, and 99% confidence bands, respectively. The PET for the same scenarios showed positive but insignificant trends in the Mann-Kendall test. Results indicate a concerning trend in the near term, with increased IWR and decreased Y_r (–20%) under SSP5-8.5 for both the crops. However, in the far future, the opposite trend has been observed.
28.	Catalytic carboxylation of sp 2 and sp 3 C–H bonds with CO 2 under atmospheric pressure conditions: An integrated experimental and theoretical study **PK Giri, P Rani, M Kaur, TJD Kumar, CM Nagaraja** - Materials Horizons, 2026 **Abstract:** The dramatic rise in CO_2 emissions from numerous anthropogenic sources is fundamentally disrupng the natural carbon cycle. Consequently, developing efficient, low-cost catalysts for effective carbon capture and utilization (CCU) as a C1 building block for the preparation of valuable chemicals and fuels will be a prominent step toward alleviating the growing atmospheric CO_2 concentration. Herein, we report the development of a two-dimensional (2D) covalent organic framework (Ag_3-TAPT-COF), constructed from an Ag(I)-based cyclic trinuclear complex (Ag_3-cluster) and a 4,4′,4″-(1,3,5-triazine-2,4,6-triyl) trianiline (TAPT) linker. Ag_3-TAPT-COF is composed of a CO_2-philic nitrogen-rich triazine ring and catalytically active Ag_3 clusters (SBUs) highly exposed in one-dimensional (1D) channels of the framework, promoting efficient CO_2 fixation through C(sp^2)–H and C(sp^3)–H carboxylation, producing corresponding high-value carboxylic acids with significant biological relevance. This work introduces a sustainable strategy employing an Ag(I)-cluster-based catalytic system for the efficient transformation of CO_2 to significant compounds through the carboxylation of inert C(sp^2)–H and C(sp^3)–H bonds, producing important commodity compounds under mild conditions. 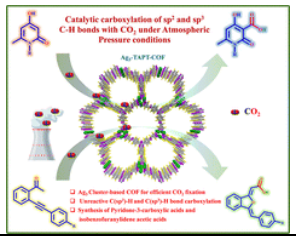
29.	Curvature-induced spin-wave dynamics in $Ni_{30}Co_{70}$ magnetic nanotubes: Angular ferromagnetic resonance, multi-mode excitation, and magnonic control **A Kumar,** V Suri, D Tiwari, B Chakraborty, VK Malik, **D Roy** - Nanotechnology, 2026 **Abstract:** Curvilinear magnetism offers a powerful route to engineer spin-wave phenomena beyond the limitations of planar architectures. In Curvilinear systems geometry itself acts as an active control parameter. Magnetic nanotubes (MNTs) represent an archetypal three-dimensional

	platform. In MNTs curvature induces emergent anisotropies, symmetry breaking, and nonreciprocal spin-wave transport without relying on interfacial Dzyaloshinskii–Moriya interactions. In this manuscript, we investigate curvature-engineered spin-wave dynamics in thick-walled $Ni_{30}Co_{70}$ magnetic nanotubes using broadband, angular-dependent ferromagnetic resonance spectroscopy. We observe pronounced splitting and hybridization of spin-wave modes that are absent in thin shells and planar films. Our measurements revealing the decisive role of finite shell thickness and curvature. The angular evolution of the spectra exhibits a maximum mode splitting near φH=60^0. These modes arises from a competition between short-range exchange and curvature-enhanced dipolar interactions. Quantitative analysis using Kittel framework results discrete spin-wave wave vectors in the range ~0.25-0.52 nm^{-1}. Observed values are in excellent agreement with existing literature based on nanotubes. Our results provide ensemble-level experimental evidence of curvature-induced lifting of mode hybridization, and spectral asymmetry in magnetic nanotubes. By establishing curvature as a robust and scalable design parameter for tailoring magnon spectra. Also, this work advances both the fundamental understanding of spin-wave physics in three-dimensional shells and the realization of reconfigurable, low-loss magnonic circuitry based on curvilinear nanomagnets.
30.	Dipole-driven ultrafast charge separation in a two-dimensional janus PtSSe/PtSTe van der waals heterostructure **P Chauhan, V Shukla, R Ahuja** - The Journal of Physical Chemistry C, 2026 **Abstract:** Understanding ultrafast interlayer charge separation in the Janus heterostructures (HSs) is crucial for photocatalytic and photovoltaic applications. In this study, we systematically investigate the electronic structure, optical response, and ultrafast carrier dynamics in a Janus PtSSe/PtSTe van der Waals (vdW) HS using first-principles calculations and nonadiabatic molecular dynamics (NAMD). The Janus PtSSe/PtSTe HS is thermodynamically stable with a reduced indirect band gap of 0.36 eV arising from interlayer orbital hybridization and dipole-induced band realignment. The planar-averaged electrostatic potential analysis demonstrates an intrinsic built-in electric field that produces a staggered type-II band alignment within the redox potential of water, which promotes spatial separation of photoexcited charge carriers. The system exhibits strong low-energy optical absorption characterized by excitonic features, which are influenced by interlayer electronic coupling. The decoherence-induced surface-hopping (DISH) approach exhibits efficient phonon-assisted charge transfer between layers, characterized by significant nonadiabatic coupling (NAC) time (5.87–9.88 meV) and a brief electronic decoherence time (τ_d) of ~96 fs. Janus PtSSe/PtSTe heterostructures possess ultrafast hole and electron transfer times of ~0.13 and ~0.97 ps, respectively, accompanied by a suppressed recombination time of ~1.03 ps. The suitable type-II band alignment, along with ultrafast recombination dynamics, showcases the Janus PtSSe/PtSTe HS as a potential candidate for optoelectronic and photocatalytic devices. 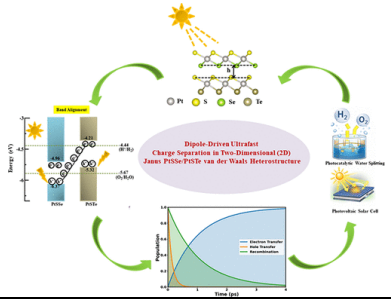
31.	Do multivariate measures anticipate traffic congestion? **SN Chattopadhyay, AK Gupta** - Royal Society Open Science, 2026

	Abstract: Traffic congestion generates substantial socioeconomic and environmental burdens, underscoring the need for reliable prediction to enable timely control interventions. This study investigates traffic jams from a critical transition perspective and assesses the predictive performance of 12 multivariate indicators across macroscopic continuum model-based and real-world data-driven scenarios. These multivariate indicators are typically based on critical slowing down (CSD) and are derived on a moving-window basis by integrating information across the three fundamental traffic variables: density, velocity and flow. The methodological framework comprises four components: sensitivity analysis, significance testing, robustness assessment and composite indicator (CI) construction. Theoretical analyses and data-driven tests show that the multivariate indicators are promising and hold substantial potential for congestion prediction. Careful selection of detrending strategies is important to remove the inherent non-stationarities in the data as their effect has been found to be non-trivial. Overall, the study bridges the application of nonlinear dynamics and the practical demands of traffic engineering. It employes universal multivariate measures that provide actionable tools for mitigating congestion and managing urban traffic efficiently.
32.	Dynamic neural architecture search for micro-expression recognition M Verma, **SK Vipparthi,** S Murala, M Abdel - Mottaleb - IEEE Transactions on Biometrics, Behavior, and Identity Science, 2026 **Abstract:** Micro-expressions (MEs) are transient in nature and reveal enough visual cues to recognize genuine emotions. Neural Architecture Search (NAS) has recently gained significant attention in the field of micro expression recognition (MER). However, existing NAS approaches in MER rely on general-purpose strategies, often reducing network depth to compensate for limited training data. This restriction can limit the discovery of optimal architectures, especially since dataset sizes in MER vary significantly. Moreover, focusing solely on operation selection and connectivity is inadequate, flexibility in depth and structure is essential to adapt to different data characteristics. While shallow networks are often considered suitable for small datasets, this assumption falls short for MER. Despite the scarcity of training samples, MEs are inherently complex, fleeting, and nuanced, requiring models with high representational power for accurate recognition. To address this trade-off, we propose a novel Dynamic Neural Architecture Search framework for MER (DNAS-MER), designed to adaptively balance model depth and architectural design based on the data. The proposed DNAS hierarchically optimizes the network depth, resolution paths, and cell-level operations through a scalable network search space and a multi-scale context-aware (MSCA) cell search space. A novel depth-aware loss function enables the model to automatically adapt depth based on data needs, while MSCA cell search, embedded with adaptive feature fusion operations, enhances ME-specific feature representation to better capture the complexity of MEs. We evaluate DNAS-MER on a composite dataset MEGC2019, CASME-II, and SMIC. Experimental results demonstrate that DNAS-MER consistently outperforms existing state-of-the-art methods for both video and image-based MER tasks.
33.	Earth pressures on underground structures in long vertical trenches with heterogeneous and nonlinear soil backfills using a slice-based numerical approach **R Ganesh** - International Journal for Numerical and Analytical Methods in Geomechanics, 2026 **Abstract:** The earth pressures on underground structures in trenches are typically evaluated using the conventional Mohr-Coulomb (MC) yield criterion under the assumption of homogeneous soil backfills. However, most geomaterials are inherently heterogeneous and exhibit nonlinear shear strength characteristics. In this research, a novel slice-based numerical solution procedure based on the limit equilibrium method of horizontal slices is developed to evaluate the earth pressure distribution in long vertical trenches backfilled with heterogeneous soils exhibiting nonlinear shear strength. The analysis is carried out under plane strain conditions

	and employs the nonlinear power-law (PL) yield criterion together with linearly varying soil parameters to account for the nonlinear and heterogeneous characteristics of the soil backfill. The variations of vertical earth pressure (σ_v) with depth (z) below the ground surface for homogeneous clay and sand trench backfills, evaluated using both the MC and PL yield criteria, reveal the significance of shear strength nonlinearity. A detailed parametric investigation is further conducted to examine the effects of different parameters on the variation of the $\sigma_v - z$ curves. The computations demonstrate that the combined effects of soil nonlinearity, heterogeneity, and arching significantly affect both the magnitude and distribution of earth pressures within the trench. Moreover, the proposed procedure yields results that show excellent agreement with those reported in the existing literature based on the MC yield criterion.
34.	Electrophotochemical asymmetric catalysis: Merging electron and photon to drive sustainable enantioselective organic synthesis **RD Thombare, P Singh, AC Shaikh** - Synthesis, 2026 **Abstract:** Asymmetric catalysis stands at the forefront of modern chemistry, serving as a cornerstone for the efficient synthesis of enantiopure chiral molecules, known for their high selectivity. In recent years, merging electrocatalysis and photocatalysis into a hybrid method called Electrophotoredox catalysis has become the focus of extensive research in organic synthesis, providing powerful and complementary strategies for constructing complex molecular architectures. This short review highlights recent advances on an emerging topic, photoelectrochemical asymmetric catalysis (PEAC) — shows potential for the efficient and sustainable production of enantiomerically enriched compounds by harnessing electron and photon in one pot. This approach facilitates efficient and sustainable redox processes for the formation of an asymmetric centre through C-H functionalization, decarboxylative functionalization, dehydrogenative cycloaddition reaction, cross-coupling, and difunctionalization of olefins.
35.	Electrothermal modeling and reliability analysis of all-carbon interconnects: An effective medium theory-based approach RK Verma…**RY Sharma** - Micro and Nanostructures, 2026 **Abstract:** The continuous scaling driven by Moore's Law has resulted in significant dimensional reductions at both the device and interconnect levels. However, conventional metal interconnects, particularly copper are increasingly challenged by performance degradation and reliability concerns at these nanoscale dimensions. Carbon-based materials such as carbon nanotubes (CNTs), graphene nanoribbons (GNRs), and graphene have emerged as promising alternatives due to their exceptional electrical conductivity, thermal performance, and mechanical robustness. In this study, we present an analytical model grounded in effective medium theory (EMT) to evaluate the electrothermal and reliability characteristics of a 11-layer carbon-based back-end-of-line (BEOL) interconnect structure at 14 nm technology node. The model incorporates composite vias composed of copper and CNTs, and GNR-based interconnects, integrated above a front-end-of-line (FEOL) structure over a silicon substrate. The analytical results are validated through finite element method (FEM) simulations using joule heating Multiphysics in COMSOL, demonstrating strong agreement between the two approaches with an error of less than 10%. We analyze the effective thermal conductivity (Keff) of the proposed BEOL architecture and quantify the temperature rise under operating conditions using image charge theory. Furthermore, reliability is assessed by estimating the mean time to failure (MTTF). Our findings indicate that the MTTF of the carbon-based BEOL structure is approximately ~ 1020 times greater than that of a conventional copper–based BEOL structure, underscoring the potential of carbon-based interconnects for nanoscale integrated circuits.

36.	Energy efficiency assessment of a hybrid transcritical CO2-compression-absorption heat pump system for heating and cooling in the dairy industry **R Beniwal,** K Garg, **H Tyagi** - International Journal of Refrigeration, 2026 **Abstract:** The dairy industry demands high energy consumption due to simultaneous heating requirements for pasteurization and cooling demands for milk storage, which is conventionally fulfilled by separate energy-intensive systems. This study presents a comprehensive comparative analysis of three combined heating and cooling systems for milk pasteurization, with emphasis on evaluating the overall energy consumption of each system. The research evaluates a conventional ammonia-based vapour compression refrigeration system (VCRS) coupled with electrical resistance heating as the baseline technology, a standalone transcritical CO_2 ($TCCO_2$) system, and a novel hybrid configuration- integrating $TCCO_2$ refrigeration system with a compression-absorption heat pump (CAHP) cycle proposed in the present study. This innovative hybrid system utilizes waste heat from the $TCCO_2$ gas cooler (GC) to drive the CAHP generator. The CAHP absorber delivers the required pasteurization temperature of 72 °C and the $TCCO_2$ evaporator provides cooling at 4 °C for milk storage. Performance analysis reveals significant energy efficiency improvements with our newly proposed hybrid system. The conventional NH_3-based system with electric heating achieves a combined coefficient of performance (COP) of 1.50, while the standalone $TCCO_2$ system demonstrates a COP of 1.22 when optimized for heating requirements, though this COP can be increased to 2.5 when excess cooling capacity is fully utilized. The proposed hybrid $TCCO_2$-CAHP system achieves the highest combined COP of 2.83, representing an 88% improvement over the baseline conventional system and consumes only 28.95 kW electrical power for processing 1 kg/s of milk, highlighting its potential as a sustainable and efficient solution for the dairy sector.
37.	Enhancement of interfacial bonding of copper and h-BN, a key to tackle the tribological tussle: Increasing the lubrication effectiveness for h-BN reinforced copper-based composites H Nautiyal, P Verma, RN Goswami, P Jha, **P Sarkar,** F Ahmad, **S Shubham,** R Tygai RKS Gautam - Materials Chemistry and Physics, 2026 **Abstract:** Copper-based self-lubricating composites are widely used in electrical and sliding components where low friction, high wear resistance, and good thermal-electrical conductivity are simultaneously required. However, low wettability and poor sinter ability characteristics of hexagonal boron nitride (h-BN) limits its use as an anti-wear material in copper matrices, leading to porosity, unstable tribofilms, and accelerated wear. The objective of this work is to overcome this interfacial incompatibility through surface functionalization and sintering-route engineering. The current study focused on to enhance the Cu–h-BN interface by synthesizing cetyltrimethylammonium bromide (CTAB) functionalized h-BN nanosheets (h-BNNS–CTAB) by an alkali-assisted hydrothermal exfoliation method. Three different types of composites were developed: CH1 (untreated h-BN, single sintered), CH2 (CTAB-functionalized h-BN, single sintered), and CH3 (CTAB-functionalized h-BN, dual sintered). Microstructural analysis (SEM, TEM, and XRD) demonstrates that CTAB functionalization significantly improves h-BN dispersion and interfacial bonding, while dual sintering further enhances densification, achieving a relative density of ~87.6%. Dry sliding tests against an EN31 steel counter face revealed that CH2 has the lowest average coefficient of friction (~ 0.12–0.18) due to the formation of a stable h-BN-rich tribofilm. CH3 has the highest hardness and the lowest wear rate (~10-4 mm3 N-1 m-1) owing to dispersion strengthening mechanism and strong metallurgical bonding between Cu and the functionalized h-BN. The analysis of worn-surface and counter face indicated that improved Cu-h-BN interfacial bonding suppresses third-body abrasion and stabilizes transfer-layer formation. These results highlighted interfacial engineering as a key strategy for designing durable copper-based tribomaterials for advanced electrical and mechanical applications.

	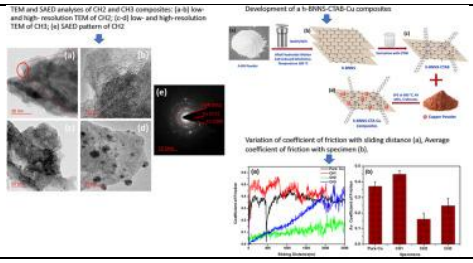
38.	Exploring semiconducting nature of atomic-level thin bismuthene nanosheets for photoredox reactions AK Singh, **S Patel,** SK Patel, **AK Mandhotra,** A Verma, V Kumar, K Kailasam, ESS Iyer, **I Chatterjee,** A Indra - ChemNanoMat, 2026 **Abstract:** Bismuthene, 2D nanosheets of bismuth with a graphene-like structure, shows semiconducting property in contrast to its semimetallic bulk form. This led us to synthesize atomic-level thin (2 nm) bismuthene nanosheets and explore its application for photoredox reactions. In the presence of light, bismuthene catalyzes the formation of aryl radical, which is efficiently utilized for the Csp^2–Csp^2, Csp^2–P, Csp^2–O, Csp^2–B, etc., cross-coupling reactions. Further, the catalyst can be recycled five times with a minimum loss of activity. The transient absorption spectroscopy reveals the underlying mechanistic aspects that govern the catalytic efficiency of bismuthene.
39.	FedHMed: Adaptive progressive loss and KL-divergence regularization for federated heterogeneous medical image classification tasks KP Singh… **SK Vipparthi,** S Murala, MS Abdel-Mottaleb - Knowledge-Based Systems, 2026 **Abstract:** Federated Learning (FL) holds promise for collaborative medical image analysis while preserving data privacy. However, its effectiveness diminishes in heterogeneous clinical environments where clients (hospitals) participate in distinct classification tasks. This task divergence, coupled with inconsistent data distributions and varying imaging modalities, introduces significant challenges such as catastrophic forgetting, noisy optimization, and instability in model convergence. These issues limit the robustness and generalizability of the global model, restricting the applicability of FL in real-world precision medicine. To address these challenges, we propose FedHMed, a novel multi-task FL framework designed to support diverse medical imaging tasks across clients. The proposed FedHMed employs a sequential model transfer mechanism that adapts to heterogeneous client tasks using a dynamic, task-complexity-aware scheduling strategy. In addition, FedHMed introduces a novel adaptive progressive loss function that adjusts learning dynamics based on the complexity of each client's task, promoting balanced model updates by mitigating noisy optimization and instability. This approach prevents overfitting and promotes efficient knowledge sharing among clients with varied data characteristics. Furthermore, we integrate Kullback–Leibler (KL) divergence regularization to counteract catastrophic forgetting and stabilize the sequential learning process in the global model. Also, label smoothing is incorporate to support loss at server side to enhance generalization and predictive calibration by mitigating overconfidence in global model predictions. Experimental results on benchmark datasets, retinal imaging, histopathological slides, and liver tumor scans, demonstrate that FedHMed consistently outperforms existing FL baselines across multiple deep learning architectures, achieving higher accuracy, stability, and adaptability in clinical diagnosis scenarios.
40.	From crystallites to columns: hierarchical Zn/Ni bimetallic MOF-biopolymer composite beads as high-capacity adsorbents for 17β-estradiol in water **A Afaq, K Chandrate, M Moirangthem, V Sharma, SK Meena, SP Gumfekar** - Chemical Engineering Journal Advances, 2026

	Abstract: 17β-Estradiol (E2) is a potent endocrine-disrupting chemical (EDC) that exists in aquatic environments and poses serious risks to human and ecological health. In this study, we synthesized a Zn/Ni bimetallic metal–organic framework (MOF) using a continuous-flow reactor and embedded it within a κ-carrageenan/NH4A matrix to prepare composite beads for efficient E2 removal from water. The anisotropic MOF crystallites exhibited a hierarchical structure and assembled into the lamellar superstructures, forming accessible adsorption sites. Small angle x-ray scattering analysis showed a radius of gyration parameter of Rg= 13.6 nm, providing an estimate of crystallite size. X-ray photoelectron spectroscopy (XPS) further confirmed the bimetallic surface composition of the Zn/Ni MOF. Batch adsorption experiments were performed to evaluate the effects of adsorbent dosage, initial E2 concentration, and solution pH. Under optimized conditions, the composite beads achieved 99.2% E2 removal with an adsorption capacity of 409.3 mg g−1. Fixed-bed column studies further showed that the Thomas model satisfactorily described the breakthrough behavior, with a maximum column capacity of 623.82 mg g−1 at a flow rate of 2 mL min−1, influent concentration of 40 mg L−1, and bed height of 20 cm. Molecular dynamics simulations further supported the strong and stable interaction of E2 with the Zn/Ni MOF framework. These results demonstrate that Zn/Ni MOF@κ-car/NH4A is an efficient, robust, and sustainable adsorbent for removing steroidal estrogens from aqueous systems. 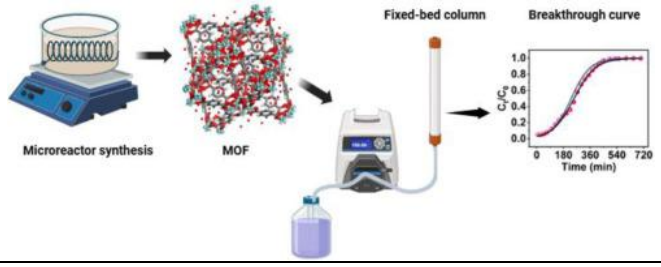
41.	Image super-resolution method based on edge-aware detail-preserving network **Inderjit, JS Sahambi** - IEEE Transactions on Emerging Topics in Computational Intelligence, 2026 **Abstract:** Super-resolution (SR) technology provides an efficient solution to meet the growing demand for high-resolution content while overcoming storage capacity constraints. Most existing SR models focus on building deeper and wider networks to achieve a high peak signal-to-noise ratio (PSNR), but often neglect critical structural and edge details. To overcome these limitations, we propose an Edge-Aware Detail-Preserving Network (EADPN) approach, which prioritizes selective local receptive features while preserving structural integrity and edge details. The proposed EADPN framework incorporates two novel components: the Variable Information Processing Block (VIPB) and the Multi-Receptive Feature Selection Block (MRFSB). The VIPB enhances contextual details by effectively processing low- and high-frequency components. Meanwhile, the MRFSB incorporates two innovative submodules: the vari-receptive fusion block (VRFB) and the variable feature boosting block (VFBB). These modules extract multi-scale, edge-oriented features, facilitating improved feature propagation and the generation of detail-enriched images. The integration of these components results in significant performance improvements. Extensive evaluations of five synthetic benchmark datasets and real-world scenarios demonstrate the effectiveness of the proposed EADPN. The results highlight its ability to enhance image quality by preserving structural fidelity and high-frequency details.
42.	Impact of climate change on potable water quality and its remediation using artificial intelligence : A review M Singh, **S Pathak,** A Hussain - Water Resources Management, 2026

	Abstract: Climate change is gradually affecting the quality, reliability and safety of potable water throughout the world. Rising temperatures, excess rainfall and changing hydrological cycles are altering the physical, chemical and biological characteristics of water sources. This in turn poses serious challenges to drinking water facilities and water distribution systems. Artificial intelligence (AI), machine learning (ML) and internet of things (IoT) have emerged as powerful tools for better water quality (WQ) monitoring, optimisation of treatment and management of infrastructure. This review is a critical assessment of the recent developments of AI-based approaches for the evaluation and remediation of drinking water quality under changing climatic conditions. It involves management of chlorination, adsorption, membrane filtration and the risk foreseen for the water distribution network in a city. The review addresses a critical gap by synthesising an integrated AI-driven framework to mitigate climate-induced WQ variability and support resilient potable water systems. It also examines the integration of AI with IoT-enabled sensor systems for real-time monitoring and predictive risk management. Furthermore, the review discusses current limitations, operational challenges, and sustainability implications of AI-based water management systems. The outcome demonstrates a growing potential of data-driven technologies to facilitate adaptive decision-making, enhance the efficiency of water treatment systems. It also portrays the resiliency of drinking water systems under climate change pressures. 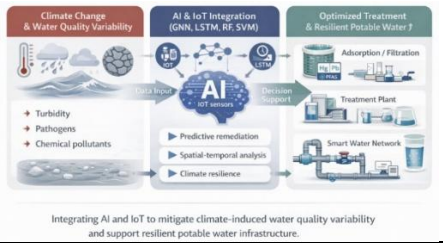
43.	Insights into 2D silicon doped γ-graphyne as an anode material in sodium-ion batteries **N Kaur, M Kaur, TJD Kumar** - Applied Surface Science, 2026 **Abstract:** 2D Si-doped *γ*-graphyne (SiG) system for applications in sodium-ion batteries (SIBs) as anode material is explored using the density functional theory method. *Ab initio* molecular dynamics simulations show that the system is thermodynamically stable at 400 K. Electronic property investigation reveals that the system is conducting and maintains its conducting behaviour after loading of Na-ion. In the charge density difference study, it has been observed that Na-ion donates 0.88 *e* of charge to the monolayer. During the adsorption of sodium ions on various sites, the twelve-membered ring is found to be the most stable site with an adsorption energy of −1.22 eV. Successive loading of Na-ion onto the monolayer indicates that 24Na atoms are stored over the 2 × 2 × 1 supercell of SiG with formula unit $Na_{24}(C_{11}Si)_4$. The system has the storage capacity of 1005.05 mAhg − 1. The convex hull is drawn using formation energies to get the most stable configurations. Moreover, the voltage profile shows average working potential of 0.55 V, which falls in the safe range. These theoretical insights confirm that the 2D Si-doped *γ*-graphyne could be a promising anode material for SIBs. 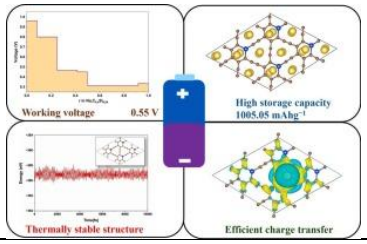
44.	Insights into the structural coexistence of hexameric states in microcrystalline insulin formulations in the solid state **KK Rohilla, Y Bhardwaj, MK Pandey** - Molecular Pharmaceutics, 2026

	Abstract: The structural complexity and insoluble nature of solid-state therapeutic proteins pose major challenges for their pharmaceutical quality control. Many conventional analytical methods cannot be applied directly to fully formulated drug products, leaving important aspects of their higher-order structure (HOS) poorly understood. In this work, we use high-resolution, proton-detected solid-state NMR (ssNMR) spectroscopy under fast magic-angle spinning (MAS) to probe the atomic-level HOS of insulin directly in its native formulated state. Recombinant human insulin powder was compared with three commercial Neutral Protamine Hagedorn (NPH) crystalline suspensions: Humulin 70/30, Insugen 70/30, and NovoMix 30. Two-dimensional (2D) $^{13}C–^{1}H$ correlation spectra showed that the overall insulin fold is conserved across all samples. In contrast, the 2D $^{15}N–^{1}H$ spectra provided a much more sensitive fingerprint of HOS and revealed clear structural differences. The amorphous insulin powder exhibits a conformationally heterogeneous ensemble characterized by a complex interplay of static disorder, dynamic averaging, and potential partial unfolding reflecting a nonhexameric, T-like architectural state. In contrast, the formulated suspensions show significantly increased ^{15}N chemical shift dispersion, consistent with more rigid, hexameric assemblies. Inspection of the allosteric reporter residues Gly^{B8} and Thr^{A8} shows that the NPH crystals are not locked into a single R_6 conformation. Instead, multiple allosteric states are present, plausibly reflecting differences in hydration and phenolic ligand binding within the lattice. The NovoMix 30 formulation (insulin aspart) exhibits further line broadening, consistent with increased lattice disorder introduced by the $Pro^{B28} \rightarrow$ Asp substitution. These observations illustrate how solid-state NMR can resolve formulation-dependent conformational heterogeneity and provide structural support for biosimilarity evaluation in solid-state protein therapeutics. 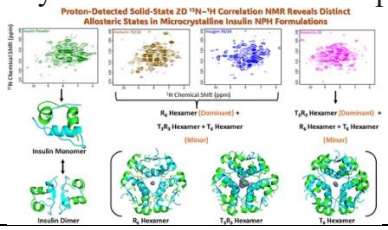
45.	Integrated machine learning and molecular dynamics for functional nanoparticle design: Synthesis, characterization, force-field development, and property prediction **M Moirangthem,** VP, **IA Fani,** C Meena, **SK Meena** - Langmuir, 2026 **Abstract:** The integration of machine learning (ML) with molecular dynamics (MD) significantly enhances the design of nanoparticles (NPs) across four key areas: synthesis optimization, advanced characterization, ML-based force fields (MLFFs), and property prediction using surrogate models. This review focuses on discrete NPs, excluding extended NPs. Traditional MD FFs often overlook essential polarization and many-body effects, while quantum methods are impractical for larger systems. In contrast, MLFFs bridge the gap between accuracy and scalability, achieving near-DFT precision for trained NP systems at computational costs approaching those of classical MD. Recent studies indicate that ML characterization can provide high morphological accuracy based on experimental imaging, and MLFFs demonstrate a close alignment with quantum reference data. However, challenges like data scarcity, model transferability, and interpretability call for collaborative efforts within the community, including the establishment of standardized benchmarks and open model repositories. This cohesive ML-MD approach enables computationally guided NP discovery for a range of applications in catalysis, energy storage, and biomedicine.

	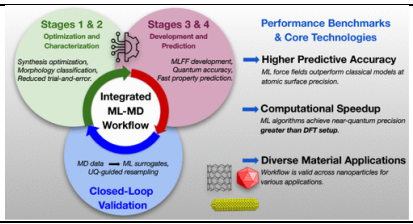
46.	Is chemical asymmetry necessary for directed motion in catalytic swimmers? **S Kumari,** C Shekhar, **A Sharma,** VR Dugyala, **V Mehandia, M Sabapathy** - The Journal of Chemical Physics, 2026 **Abstract:** In the context of directed motion or self-propelled catalytic swimmers, a central open question is whether Janus-type chemical asymmetry is essential for inducing self-propulsion. However, to tackle this unresolved puzzle, we demonstrate that anisotropic catalytic colloids, possessing chemically homogeneous surface activity but asymmetric geometry, exhibit sustained non-equilibrium propulsion, biasing Brownian dynamics toward directed motion. Self-propelled anisotropic colloids provide a versatile platform for investigating non-equilibrium transport and collective dynamics in active matter systems. Shape anisotropy introduces additional degrees of freedom that strongly influence propulsion mechanisms and self-assembly in bulk suspensions. Here, we report the synthesis of anisotropic platinum-coated polystyrene (PS–Pt) particles with an acorn-like geometry (1 μm) using a temperature-induced deformation approach. We examine the propulsion and collective behavior of these acorn-shaped particles in their monomeric, dimeric, and trimeric forms whose pronounced geometric asymmetry distinguishes them from Janus colloids. Self-propulsion is driven by the asymmetric catalytic decomposition of hydrogen peroxide on the platinum-coated region, resulting in sustained translational motion. The curvature anisotropy of the acorn geometry generates uneven solute gradients and induces motion. Statistical analyses based on Gaussian and non-Gaussian displacement distributions confirm the active nature of the observed transport and elucidate the flow behavior of both individual particles and self-assembled structures.
47.	Life cycle assessment of energy and CO_2 emission in clinker, OPC, and PPC production: case studies and pathways to emission reduction **B Sharma, AS Rajput,** S Barbhuiya - Innovative Infrastructure Solutions, 2026 **Abstract:** Cement production remains a highly energy-intensive process and a major contributor to global CO_2 emissions, particularly in emerging economies such as India. This study presents a comprehensive life cycle assessment (LCA) of energy use, carbon emissions, and resource utilization associated with the production of clinker, ordinary portland cement (OPC), and Pozzolana portland cement (PPC) at two representative Indian cement plants. The assessment is based on detailed plant-level operational data covering all major production stages, thereby providing India-specific, process-level insights beyond conventional reliance on generic international databases. Also, by integrating primary plant-specific data with process-wise LCA and scenario-based analysis, this study offers a more realistic evaluation of energy and emission drivers in the Indian cement industry. Results indicate energy intensities of 4568.96–4063.59 MJ/tonne for clinker, 4310.95–3886.58 MJ/tonne for OPC, and 3311.22–2994.67 MJ/tonne for PPC. Corresponding CO_2 emissions range from 1023.66 to 967.22 kg/tonne (clinker), 959.56 to 913.87 kg/tonne (OPC), and 676.22 to 637.48 kg/tonne (PPC). Compared to global benchmarks, OPC production in India consumes 12.73% more energy and emits 18.59% more CO_2, highlighting significant efficiency gaps within the sector. Scenario-based assessments indicate that clinker substitution and alternative fuel adoption can reduce emissions by up to 70%, demonstrating substantial potential for decarbonization. The findings

	provide actionable insights for industry and policymakers, supporting the implementation of low-carbon strategies and enhancing the sustainability of cement production in India.
48.	Linking terrain attributes and land use land cover dynamics with past and future landslide susceptibility trends K Khusulio, R Kumar, **S Sharma,** K Singh, **RK Tiwari** - Geological Journal, 2026 **Abstract:** This work delves into the assessment of 12 selected terrain factors responsible for landslides in the Mao Maran region of North-East Himalaya in India and includes a comparative study of the 2020 landslide susceptibility map (LSM) with a projected 2030 LSM. The terrain factors considered in this study are land use and land cover (LULC), stream power index (SPI), geology, 7aspect, relative relief, soil, profile curvature, road buffer, topographic wetness index (TWI), drainage buffer, fault/fold/thrust (FFT) and slope. A detailed investigation of how the selected terrain factors influence landslides in the study area was conducted using the weight of evidence method and the final LSM was generated using a random forest model. Future LULC map simulation was done using the artificial neural network cellular automata model (ANN-CA). Additionally, LULC maps for the years 2000, 2010, 2020 and 2030 were generated to identify differences in physical parameters over time. Change detection revealed a decrease in dense forest classes and an increase in scrubland, settlement, and barren land classes. LSM maps for 2020 and 2030 were generated using the receiver operating characteristic (ROC) curve, with prediction accuracies of 88.1% for 2020 and 85.5% for 2030. The LULC factor played a significant role in influencing landslides, and changes in LULC inferred a substantial impact on the landslide conditioning scenario. This research can be useful for planning, mitigation, and development activities in the study area.
49.	Magnetically induced high Q quasi-bound state in the continuum mode via fundamental lattice mode coupling in complementary terahertz metasurface S Adhikary…**G Kumar** - Journal of Applied Physics, 2026 **Abstract:** Metasurfaces have emerged as powerful platforms for controlling electromagnetic waves through field confinement and resonance engineering. This work investigates the interplay between magnetic field-driven quasi-Bound State in the Continuum (quasi-BIC) resonance and lattice mode coupling in a complementary metasurface comprising coupled bar resonators. By introducing opposite tilts in the bar resonators, we observe the emergence of sharp resonance resulting from anti-symmetric current distributions, forming a quasi-BIC mode with strong field confinement. It is observed that the strategic change in periodicity significantly enhances the quality factor of the resonance, reaching maximum when the quasi-BIC mode couples to the fundamental lattice mode. We performed terahertz time domain spectroscopy of the fabricated samples and observed that the results are consistent with simulations, further confirming a strong interaction between the modes. These findings opens up an avenue for designing high-Q low loss metasurfaces with potential applications in sensing, filtering, and terahertz photonic devices.
50.	Magnon valley-orbital hall effect driven by surface acoustic waves in two-dimensional honeycomb antiferromagnets **M Faizee, A De Sarkar** - Physical Review B, 2026 **Abstract:** The magnon orbital Hall effect in two-dimensional (2D) honeycomb antiferromagnets driven by pseudogauge fields induced by surface acoustic waves (SAWs) has been investigated. Unlike previous studies where the orbital Hall response of magnons was primarily driven by temperature gradients, we demonstrate that strain-induced pseudoelectric fields generated by Rayleigh-type SAWs can also induce a finite magnon orbital Hall current. In the absence of Dzyaloshinskii-Moriya (DM) interaction, the contribution originates solely from the valley-independent pseudoelectric field E_1^s, whereas the valley-contrasting field E_2^s gives no net

	contribution. When the DM interaction is introduced, the valley degeneracy in the magnon bands is lifted, leading to a population imbalance between the K and K valleys, which activates additional contributions from E_2^s, and consequently modifies the anomalous orbital Hall conductivity of magnons. Our results reveal a distinct mechanistic pathway to control magnon orbital transport using SAWs, offering opportunities for valley-orbitronics and magnonic device functionalities in 2D magnetic systems.
51.	ME-NAS: A micro expression feature adaptive neural architecture search M Verma, **SK Vipparthi,** S Murala, M Abbel- Mottaleb - ACM Transactions on Intelligent Systems and Technology, 2026 **Abstract:** Convolution neural networks (CNN) have emerged as a prevailing paradigm for micro-expression recognition (MER) yet, it is inefficient and time-intensive to design optimal CNN-based MER models manually. In recent times, the neural architecture search (NAS) has garnered attention due to its automatic CNN architecture searching ability. However, the performance of NAS in MER is limited by challenges such as rapid duration, subtle intensity, and a mismatch between architecture and cell-level search. The existing search space, which stacks 12 cells with 3 transition paths (down sample, up sample, and same resolution), creates deep networks that may diminish minute spatiotemporal features due to progressive convolution and pooling. Therefore, motivated by these factors, in this article, we introduce a novel approach, the Micro-Expression Feature Adaptive NAS (ME-NAS), to analyze true human emotions through MER. While NAS has gained attention for its automatic CNN architecture search ability, its application in MER faces challenges due to ingrained challenges (rapid duration, subtle and low intensity) and the discrepancy between architecture and cell-level search. The existing NAS architecture search space is designed by stacking 12 cells with 3 transition paths (down sample, up sample, and same resolution), resulting in a deep network. Such deep networks may diminish minute spatiotemporal features due to the progressive convolution and pooling operations. Motivated by these factors, we designed a new NAS algorithm: ME-NAS. The ME-NAS comprises f (EXPERT) in architecture search, along with refined and complementary feature derivative (ReCODE) operations in cell-level search. The EXPERT aims to trace the optimal paths instead of covering all possible paths between cells. The ReCODE operations capture micro-level variations from spatial and temporal domains by introducing 24 3D convolution operations. The proposed ReCODE and EXPERT search space jointly lead to the search for a robust and shallow CNN architecture for micro-expressions (MEs). The proposed ME-NAS is evaluated on six datasets: CASME-I, CASME-II, CAS(ME), SAMM, SMIC, and MEGC-19 composite, with two evaluation strategies: LOSO and cross-domain, respectively. The experimental results manifest that the proposed ME-NAS outperformed the state-of-the-art approaches on both evaluation strategies.
52.	Metric number theory of fourier coefficients of Hilbert modular forms S Kaushik, **B Kumar** - International Journal of Number Theory, 2026 **Abstract:** In this note, we attempt to generalize the work of Bengoechea (2019) to the case of Hilbert cusp forms. We prove Diophantine approximation of a real number by Fourier coefficients (supported at prime powers) of a primitive Hilbert cusp forms and we compute the density of such prime ideals. We also study ssthe refined rate of approximation of real numbers by Fourier coefficients of primitive Hilbert cusp forms, using techniques and results from metric number theory such as Schmidt's game and metrical inhomogeneous Diophantine approximation.
53.	Morphine dependence vaccines: Advances, challenges, and future directions **MS Dadwal, JA Malik, JN Agrewala** - Current Pharmaceutical Biotechnology, 2026

	Abstract: Morphine is a psychoactive drug that has been commonly used for the past many decades for medicinal purposes in public health departments. However, prolonged use leads to dependence, tolerance, and addiction. In order to address these issues, medications such as naloxone, naltrexone, and buprenorphine are utilized as anti-dependence drugs. In some cases, it has been seen that people face effects like sleep deprivation and issues related to the gut, and if taken in excess, it can have the same effect as dependence. This review discusses the latest developments in treatments for morphine dependence, including vaccine-based immune-therapies, nanotechnology-enhanced delivery systems, gene-regulatory techniques, and computational models of receptors. This comparative analysis highlights that vaccine designs based on TLR-targeted therapy, nanoparticle-enhanced therapy, and modulation of the DARPP-32 gene all play a crucial role in significantly diminishing morphine's major effects and altering reward-related signaling. The vaccines generate these anti-morphine antibodies and support immune memory functions, such as incorporating adjuvants like Pam3Cys, multivalent designs that address multiple opioids, and approaches using gold nanorods for gene delivery, further boosting vaccine effectiveness. Some approaches have even demonstrated the capacity to modulate brain pathways involved in dependence. Although clinical trials are still waiting for morphine-targeted therapy, the preclinical stage shows quite promising results and needs to be considered for therapy purposes. Collectively, these methods offer a cohesive, up-to-date perspective on novel strategies, emphasizing key mechanistic factors, and demonstrating how this review goes beyond earlier analyses focused on opioids.
54.	Nanobubbles by hybrid electro-membrane method: ROS quantification and utilization in complex wastewater treatment **G Yadav, H Sharma, N Dutta, K Rajawat, A Sonowal, N Nirmalkar** - Journal of Hazardous Materials, 2026 **Abstract:** Nanobubbles (NBs) possess unique interfacial properties that enhance gas-liquid reactions and radical generation, making them promising for intensifying advanced oxidation processes (AOPs). However, the mechanistic understanding of reactive oxygen species (ROS) generation across different NB generation strategies and its impact on treatment performance remains limited. In this study, major NB generation methods were systematically compared in terms of NB characteristics, gas-liquid mass transfer, and ROS production using fluorescence-based diagnostics. Electrochemically reactive nanobubbles (ERNBs) exhibited the highest ROS activity, generating hydroxyl radicals (OH·), superoxide radicals (O2·−), and hydrogen peroxide (H2O2), while membrane-derived CO2 NBs produced moderate OH· and oxygen-, nitrogen-, and air-based NBs yielded detectable H2O2. While ERNBs showed high intrinsic ROS productivity, their mass-transfer capability was limited, whereas membrane-based NBs provided high mass-transfer with lower ROS yields. To integrate these complementary advantages, a hybrid electro-membrane nanobubble (HEM-NB) system was engineered, achieving higher NB density, enhanced mass transfer, and increased ROS availability. Application studies using tannic acid (TA) as a representative polyphenolic contaminant in single and complex textile-like matrices demonstrated improved degradation kinetics, with synergy factors of ∼1.33 and ∼1.23 compared to ERNBs-only treatment. Overall, this work establishes mechanistic-performance linkages and demonstrates the oxidative robustness of hybrid NB technology under chemically complex effluent treatment.

	
55.	Nature-inspired hybrid photocatalytic system for degradation of persistent organic pollutants, including pharmaceutical remains using solar-driven continuous flow reactor **S Jaswal, R Devi, A Singh,** N Kaur, **N Singh** - Chemistry-An Asian Chemical Editorial Society, 2026 **Abstract:** Sunlight-driven photocatalytic reactors for wastewater treatment have become a growing hot topic among researchers owing to their inexpensiveness, scalable potential, and minimal ecological impact. Herein, we have utilized 3D printing to fabricate a packed bed reactor (PBR) consisting of an open serpentine channel packed with zinc oxide nanoparticles (ZnO) coated onto silica nanoparticles (SiO_2) incorporated on cellulose nanocrystals (CNC) that is ZnO@SiO_2@CNC. This developed PBR overcomes the expensive and time-consuming limitations of batch reactors with continuous flow mass treatment of persistent organic pollutants, including methylene blue (MB), Congo red (CR), and ciprofloxacin (CIP). The PBR exhibits remarkable removal efficiency that is further enhanced with increasing turbulence, reaching 99% and 98% for MB and CR, respectively, in just 20 min. Moreover, its potential for the photocatalytic degradation of the CIP antibiotic drug was confirmed with a removal efficiency of 81% in 110 min. The hybrid system was further explored for single-run operation and showed a degradation capacity of 99% for both MB and CR. The nanocomposite applicability to degrade these dyes at different pH levels and degradation pathways was also analyzed. Additionally, similar performance in degrading these persistent pollutants spiked in tap and river water confirmed its environmental applications for real samples.
56.	Neuroligin-3: A novel exercise-induced secreted factor enhancing insulin sensitivity in obese insulin-resistant mice A Sinha, **D Patra,** S Mishra, **A Vashisth,** S Sharma, U Dey, **P Ramprasad, S Roy,** A Kumar, K Tikoo, **D Pal,** S Dasgupta - Diabetes, 2026 **Abstract:** The salutary effects of physical exercise in mitigating metabolic disorders, particularly type 2 diabetes, are well recognized. Several studies have demonstrated that endurance training boosts the production of exercise-induced myokines, which are pivotal for interorgan communication enhancing insulin sensitivity. However, several challenges, including an incomplete understanding of underlying molecular mechanisms, hinder their therapeutic application. Here, we have identified a potential exercise-induced mediator, neuroligin-3 (NLGN3), that enhances insulin sensitivity and abrogates inflammation. Mechanistic studies in white adipocytes revealed that NLGN3 interacts with neurexin-3 (NRXN3) to modulate their function and insulin sensitivity, while in macrophages, NLGN3 engages with NRXN1 to attenuate inflammation and promote an anti-inflammatory phenotype. Administration of NLGN3 in high-fat diet (HFD)–fed mice significantly ameliorated obesity-induced visceral adipose tissue dysfunction and insulin insensitivity; however, these attributes are markedly abolished in NRXN1/3-deficient mice. In addition, elevated serum NLGN3 levels following swimming exercise training correlated with improved metabolic outcomes in HFD-fed obese diabetic mice. These findings suggest that NLGN3 may serve as a key mediator of exercise-induced metabolic benefits and highlight the NLGN3-NRXN1/3 pathway as a promising target for managing obesity-induced insulin resistance. Article Highlights: This study aimed to identify novel exercise-induced myokines and their role in improving insulin sensitivity and reducing

	inflammation. We identified neuroligin-3 (NLGN3) as an exercise-induced mediator that enhances insulin sensitivity and alleviates inflammation. Exercise-induced NLGN3 upregulation or recombinant NLGN3 administration improved metabolic function in high-fat diet–fed mice via neurexin-1 and -3 (NRXN1/3), but these benefits were lost upon NRXN1/3 ablation. NLGN3 emerges as a key mediator of exercise-driven metabolic benefits and a promising therapeutic target for obesity-associated insulin resistance. 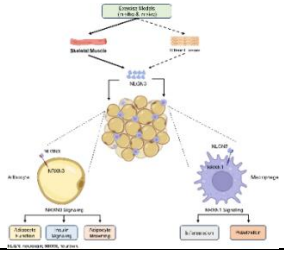
57.	Nonconserving locally disordered exclusion process under constrained resources **N Sharma,** B Pal, A Gupta, **AK Gupta** - Physical Review E, 2026 **Abstract:** Driven by transport processes in natural and man-made systems, we examine a locally disordered totally asymmetric simple exclusion process with Langmuir kinetics in a resource-constrained environment. The disorder is in the form of a defect that may bind to or unbind from a particular site and slows down the particle movement, when present on the lattice. Using a mean-field approach, we analyze the steady-state behavior of the model by computing density profiles and constructing phase diagrams in the parameter space, thereby revealing a rich quantitative and qualitative phase structure. The impact of finite resources and Langmuir kinetics on the stationary properties of the system is analyzed by varying the filling factor and binding constant. Upon varying the filling factor, the results uncover several critical values where the phase diagram changes qualitatively and the resulting phase complexity varies nonmonotonically. As the binding constant is increased from small values, the phase structure evolves from a limited set of phases to maximal diversity at moderate values, before settling into a simplified regime at large values. An obstruction factor is introduced to capture the combined effects of defect density and the slowdown rate in order to incorporate the role of the dynamic defect. Owing to this combined effect, increasing the obstruction factor simplifies the phase diagram, suppressing Meissner-type phases and promoting high density and shock regimes. The mean-field predictions are verified through Monte Carlo simulations implemented via Gillespie algorithm.
58.	Optical control of charge environments in nanodiamonds for enhanced quantum sensing stability **R Dhankhar,** DBR Dasari, **RV Nair** - Physical Review A, 2026 **Abstract:** Nitrogen-vacancy (NV) centers in nanodiamonds are promising platforms for nanoscale quantum sensing in biological and condensed-matter environments, but their performance is often limited by charge-state instability and strain-induced spectral fluctuations. Using spin-state-dependent emission measurements, we demonstrate that controlled optical excitation can stabilize the local charge environment surrounding the NV centers in nanodiamonds, thereby improving sensing stability. We observe that spin-state-dependent spectral emission linewidth and splitting saturate as a function of excitation laser power density, which correlates with a reduction in charge fluctuations across nanodiamonds with varied sizes and impurity concentrations. To elucidate these measurements, we develop a macroscopic theoretical model that reproduces the ensemble-averaged response of large NV populations without requiring explicit simulation of microscopic charge dynamics. Furthermore, we introduce incoherent sensing protocols that exploit environmental noise to achieve sensitivity of $\mu\times$T/√Hz, even in regimes of strong spin decoherence. These results provide a practical route

	to enhancing the robustness of NV-based quantum sensors and an optically addressable platform for physically unclonable imaging tags relevant to quantum security and anticounterfeiting applications.
59.	Performance enhancement and emergence of self-powered in amorphous Ga2O3 solar-blind photodetectors via controlled reducing-environment annealing **R Dahiya, P Rani, L Rani, M Kumar** - Applied Surface Science, 2026 **Abstract:** Solar-blind photodetectors (SBPDs) based on a-Ga_2O_3 have attracted considerable interest due to their room-temperature growth and scalability. However, device performance is often constrained by structural disorder and defect-related carrier trapping. Post annealing under different environments has been widely adopted as an effective approach to mitigate structural disorder and regulate defects. Herein, we investigate the effect of post-annealing under a controlled sulfur-rich reducing environment on the structural, chemical, and optoelectronic properties of a-Ga_2O_3-based SBPD. Structural analysis reveals a phase transformation from a-Ga_2O_3 to polycrystalline β-Ga_2O_3 at optimum sulfur content, while excessive sulfur results in the formation of an ultrathin Ga_2S_3 surface layer. These results reveal that optimal sulfur annealing promotes crystallization and regulates oxygen vacancies. The device annealed with an optimal sulfur amount exhibits a ~26-fold enhancement in responsivity compared to the unannealed device while maintaining a comparable response time. Notably, this optimized device also demonstrates stable zero-bias photo response with a high photo-to-dark current ratio of ~4.1×10^4 and a fast fall time of 150 ms, along with excellent long-term stability under ambient conditions. These results establish a controlled reducing-environment annealing as a simple and effective strategy to enhance the performance of a-Ga_2O_3-based solar-blind photodetectors and enable self-powered operation. 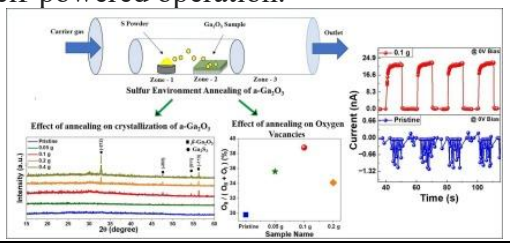
60.	Performance evaluation of natural rubber latex treatment across various sand types for seismic energy dissipation **S Sharma, N James,** U Veena - Soil Dynamics and Earthquake Engineering, 2026 **Abstract:** Large amount of seismic energy released during earthquakes is dissipated through particle rearrangement in saturated sands. This process generates excess pore water pressure in undrained conditions, which may lead to liquefaction. The present study aims to determine the degree of improvement for liquefaction mitigation after natural rubber latex (NRL) treatment for different sands through energy dissipation framework. In this study, total of five sand types was utilized, comprising river sands procured from the banks of the Sutlej and Yamuna Rivers, in addition to three locally sourced clean sands of different grades. Untreated and NRL treated specimens of 100 mm height and 50 mm diameter are prepared at 40% relative density. Pressurized fluid permeation setup is used for permeating NRL through sand specimens. A series of constant volume cyclic triaxial tests were conducted at 1Hz frequency in stress-controlled mode at different cyclic stress ratios (0.20, 0.25, 0.30 CSR) and strain-controlled mode at different strain amplitudes (0.3%, 0.5%, 0.7%). Test results show enhancement for capacity energy for different sands after NRL treatment. A new parameter, Stabilization Efficiency Index (SEI) is proposed to evaluate the degree of improvement in terms of capacity energy brought by NRL treatment. SEI increases from 10 to 40 as the effective size of sand particles increases from 0.077 mm to 0.9 mm. Additionally, the degradation of shear modulus in NRL-treated specimens

	was significantly less compared to untreated specimens. SEM images confirm that different porous structures in different sands affect the formation of rubber strand network. Strong network of rubber strands is formed in presence of sufficient intergranular void space. By improving the energy dissipation mechanism for a soil layer, NRL treatment of sand emerges as an innovative solution for enhancing the liquefaction resistance of structures in earthquake prone regions.
61.	Psych-Air: Predictive smog analytics for psychotic disorder patients' risk assessment in smart cities **S Dey,** AS Prasad, **S Mishra,** D Ramesh - IEEE Internet of Things Journal, 2026 **Abstract:** The issue of smog in smart cities (SCs) poses serious health risks due to the rising concentrations of air pollutants (APs), including particulate matter, carbon, and sulfur. Their complex and dynamic behavior makes data-driven analysis challenging. Thus, accurate source identification and forecasting of those APs are vital for assessing psychotic disorder risks in hospitalized patients. To address this, a model named Psych-Air has been proposed. The proposed Psych-Air model employs federated learning (FL) with a customized multivariate bidirectional GRU (BGRU) architecture featuring cross-variable gated attention and parallel temporal encoders. Unlike conventional FL schemes, Psych-Air incorporates heterogeneity-aware and pollutant-sensitive federated optimization, enabling stable and communication-efficient learning across non-IID smart city environments. It also models pollutant and meteorological time series as an interdependent tensor stream, with dynamic gating and synchronized bidirectional states capturing pollutant-specific patterns. A shared fusion layer learns spatiotemporal signatures predictive of psychotic disorder onset while operating securely in a decentralized environment. Psych-Air effectively isolates latent triggers from noisy environmental data, achieving clinically relevant forecasting. FL-based BGRU identifies key pollutant sources, accounting for 46% of Air Quality Index impact in SCs. The model outperforms traditional ML, DL, and FL methods by 20%, 15%, and 10%, respectively, and supports the assessment of psychotic disorders through statistical analysis. Additionally, Psych-Air promotes sustainable, energy-efficient smart cities by reducing annual costs and CO emissions, proving adaptable across various urban settings.
62.	Rate-induced tipping in Savanna–forest ecosystems: Effects of fast-varying fitness parameters in the framework of compactification **R Kumar K, PS Dutta** - Royal Society A: Mathematical, Physical and Engineering Sciences, 2026 **Abstract:** Savannas are grass-dominated ecosystems with scattered shrubs and savanna trees, often coexisting with tropical forests. They host a diverse range of plants and animals, act as a major carbon sink, regulate the global climate and support local economies. However, rapid environmental change is degrading these ecosystems, ultimately leading to a decline in biodiversity. Here, we consider a mathematical model of savanna–forest ecosystems to investigate rate-induced tipping (R-tipping) between distinct states under rapid variations in fitness parameters of different functional types (i.e. grass, savanna saplings and adult trees and forest trees) over time. To establish the existence of R-tipping, we determine basin instability (BI) in the corresponding frozen system with fixed-in-time inputs. Since time-dependent parameters make the model non-autonomous, it lacks compact invariant sets, which preclude the use of classical bifurcation theory. To address this, we reformulate the non-autonomous system with bi-asymptotically constant inputs as an autonomous one using compactification with an additional bounded variable. Furthermore, compactification enables us to identify the R-tipping threshold, which is crossed when tipping occurs. Overall, our analysis reveals distinct rate-induced transitions, including shifts to dominant states of grass, adult savanna trees and oscillatory dynamics.

63.	Rearrangement of donor–acceptor cyclopropanes for the synthesis of substituted cyclopentene derivatives **C Laru, A Hazra, P Banerjee -** The Journal of Organic Chemistry, 2026 **Abstract:** The rearrangement of donor–acceptor cyclopropanes has been demonstrated for the first time using Brønsted acid catalysis. A series of substituted cyclopentene derivatives were obtained in moderate to good yields and moderate diastereoselectivities. Further control experiments and synthetic applications have also been carried out. 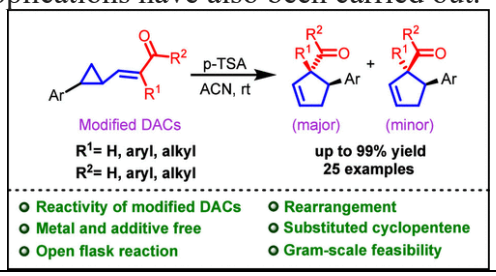
64.	Red photon-driven aminomethylation of indoles to access the sterically hindered indolyl tertiary amines **N Lal, SS Bisht,** MV Mane, **SP Gumfekar, AC Shaikh** - Green Chemistry, 2026 **Abstract:** Introducing the amine functionality to readily available feedstock chemicals is an effective strategy to rapidly enhance the molecular complexity and access valuable scaffolds. Herein, we have developed a red photon-driven *N*-aminomethylation of indoles utilizing a ^{n}PrDMQA^{+} organic photocatalyst. Under red-photon irradiation, amine radical cations exclusively generate less hindered iminium species, which are then sequentially converted into sterically crowded tertiary amines of interest in organic synthesis, enabling a high-yield *N*–C(sp^3) coupling reaction under mild conditions. This protocol demonstrates a broad substrate scope, allowing late-stage modification of bioactive natural compounds and pharmaceuticals under mild conditions. Control experiments and DFT studies on transient intermediates confirmed the mechanistic pathway, highlighting the generation of a kinetically favored iminium ion to generate a library of aminated indole derivatives.
65.	Role of stent geometry on net-shape fabrication of bioresorbable polymeric coronary stent via microinjection molding **DK Tyagi, DK Mahajan** - International Journal of Precision Engineering and Manufacturing, 2026 **Abstract:** Bioresorbable polymeric coronary stents (BCSs) offer transformative potential for cardiovascular therapy by providing temporary vascular support before degrading, yet structural performance and complex processing hinder their clinical translation. Single-shot net-shape fabrication via micro-injection molding (μIM) offers a cost-effective, high-throughput solution with minimal material waste in cleanroom settings. To overcome mold underfilling in high L/t ratio (> 650) geometries, this study introduces a multiphysics computational framework combining finite element analysis for structural validation with computational fluid dynamics for melt-flow simulation. The objective is to optimize BCS designs for mechanical integrity and manufacturability, enabling scalable μIM-based net-shape production. The framework systematically evaluates seven BCS designs, including four CE-marked geometries, two patented novel variants, and one reported design under uniform processing conditions using different grades of PLA. Structural parameters including radial strength, bending resistance, and elastic recoil, were analyzed alongside manufacturability outcomes such as mold-filling efficiency, pressure requirement, and defect formation. Key findings reveals that the manufacturability via μIM depends not only on L/t ratio and gate configuration but also on the detailed geometric

	profile of the stent. Intricate designs demand prohibitively high injection pressures (~ 1500 MPa) due to extremely fine features and impractical profiles which impeding melt propagation, whereas the patented Diamond-4 geometry achieves comparable radial strength, lower elastic recoil, and slightly higher bending stiffness, with complete cavity filling at substantially lower injection pressures and the least shrinkage among all evaluated designs. Coupling structural and melt flow analysis, the methodology links clinical needs like vascular patency and endothelialisation with µIM process challenges including high polymer viscosity, premature solidification, and demolding issues. This dual-validation approach aligns mechanical performance with processing constraints, offering a predictive tool for net-shape fabrication of next-generation polymeric BCS. It minimizes costly experimental trials and accelerates scalable stent development.
66.	Room temperature photochemical synthesis of metal–organic frameworks for enhanced photocatalysis Y Wang, J Guan, **K Kumar,** W He…**SK Meena…**D Ma - Nature Communications, 2026 **Abstract:** The function of metal–organic frameworks (MOFs) is fundamentally governed by their synthesis precision. Here, we report a light-driven strategy enabling ambient-temperature MOFs synthesis (15 °C, 4 hours) for cobalt-porphyrin frameworks (phoPPF-3), overcoming traditional thermal constraints. This approach achieves multidimensional control, manifested in two-dimensional hourglass morphologies and selective Co^{2+}-carboxylate coordination that preserves free-base porphyrin cores unattainable conventionally. Resulting phoPPF-3 exhibits enhanced thermal stability and higher photocatalytic activity in benzyl alcohol oxidation and H_2 evolution comparing to solvothermal analogues. The methodology demonstrates a certain generality through successful extension to other MOFs. This work marks the demonstration of using photons to initiate and guide MOFs synthesis and establishes a sustainable approach for atomically precise MOFs engineering via photochemical control.
67.	Some aspects of vector valued de branges spaces of entire functions **S Mahapatra, S Sarkar** - Computational Methods and Function Theory, 2026 **Abstract:** This paper deals with certain aspects of the vector valued de Branges spaces of entire functions that are based on pairs of Fredholm operator valued functions. Some factorization and isometric embedding results are extended from the scalar valued theory of de Branges spaces. In particular, global factorization of Fredholm operator valued entire functions and analytic equivalence of reproducing kernels of de Branges spaces are discussed. Additionally, the operator valued entire functions associated with these de Branges spaces are studied, and a connection with the operator nodes is established.
68.	SPIM RSMA: Prototyping and experimental validation of its superiority over traditional RSMA **S Bhattacharyya, S Kumar, S Darshi,** K Singh - IEEE Wireless Communications Letters, 2026 **Abstract:** In this letter, we develop and implement a transceiver prototype for split-packet interference management in an uplink rate-splitting multiple access (SPIM RSMA) framework using a software-defined radio (SDR) platform. The primary objective is to experimentally validate the performance superiority of the SPIM RSMA framework over conventional uplink RSMA and non-orthogonal multiple access (NOMA) schemes. Experimental results demonstrate that SPIM RSMA achieves significantly improved bit error rate (BER) and throughput performance compared to traditional RSMA and NOMA. These gains are primarily attributed to the effective mitigation of split packet interference (SPI), which preserves the inherent advantages of rate splitting. Furthermore, the experimental BER results are corroborated through comparisons with simulation-based results, thus validating the proposed transceiver architecture.

69.	Structural, optical, photocatalytic and antibacterial properties of hydrothermally synthesised CuO–WO3 heterojunction nanocomposite RP Jakkula, D Suresh, **SR Konda,** R Raghavapuram - Asian Journal of Chemistry, 2026 **Abstract:** Nanostructured pure CuO and CuO-WO_3 heterojunction composites were synthesised using a hydrothermal technique. The materials were analysed by XRD, SEM, TEM, AFM, EDX and FTIR to determine their physico-chemical properties. Monoclinic crystal structure and heterojunction composite that developed between the synthesised CuO and WO_3 are indicated. The photocatalytic activity was investigated *via* the degradation of methylene blue under visible light, where the CuO–WO_3 nanocomposite exhibited higher photocatalytic activity compared to the unmodified nanostructured CuO. The enhanced photocatalytic activity of the composite material is attributed to the suppressed recombination of photogenerated electron–hole pairs under visible-light irradiation and the increased generation of reactive oxygen species (ROS) facilitated by the presence of WO_3. The antibacterial performance of the prepared materials was evaluated against Gram-positive and Gram-negative bacteria. In comparison to unmodified CuO, the CuO–WO_3 nanocomposite demonstrated superior antibacterial activity due to better surface deposition and ROS-mediated bacterial cell membrane destruction, which was attributed to the interaction of the generated ROS with the cell membranes of bacteria. The enhanced performance is attributed to improved interfacial charge transfer, heterojunction-induced carrier separation and increased surface-active sites. The CuO–WO_3 system demonstrates the significance of interfacial engineering and phase coupling in tailoring functional properties. These findings highlight the potential of such oxide-based composites as multifunctional agents for advanced environmental and antimicrobial applications.
70.	Suitability and compatibility study of UHMWPE for heart valve applications A Kumar…**C Sasmal,** CK Raul, SS Banerjee - Polymer-Plastics Technology and Materials, 2026 **Abstract:** Polymeric heart valves have emerged as promising class of next-generation prostheses, offering combined advantages of mechanical durability and biological compatibility. However, long-term success of such valves depends critically on selection of suitable polymeric materials that can endure repetitive mechanical stresses while maintaining excellent hemocompatibility. In this context, ultra-high-molecular-weight polyethylene (UHMWPE) has gained attention due to its excellent wear resistance, high toughness, low friction coefficient, chemical stability and biocompatibility. The present study investigates the suitability and compatibility of UHMWPE for heart valve applications, emphasizing its thermal, dynamic mechanical, hemocompatibility and antithrombogenic characteristics. Thermal analyses confirmed the high thermal stability and semi-crystalline (~41%) nature of UHMWPE well beyond physiological temperatures, while dynamic mechanical analysis at body temperature (37°C) revealed a predominantly elastic response with low energy dissipation under frequency and strain-controlled loading. Hemolysis testing demonstrated a hemolytic ratio of 1.5%, confirming UHMWPE's non-hemolytic behavior. Blood smear formation analysis revealed no evidence of smear or blood film on the surface, indicating an antithrombogenic nature. Furthermore, platelet adhesion studies showed remarkably low platelet adhesion density, affirming UHMWPE's ability to minimize platelets adhesion and prevent thrombus formation. 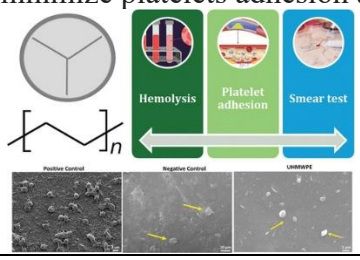

71.	Torsional amplification factors for floor response spectra in buildings with nominal torsion A Jain, **M Surana** - Earthquake Spectra, 2026 **Abstract:** This study investigates the impact of nominal building torsion on characteristics of floor acceleration response spectra. To achieve this objective, a set of 16 reinforced-concrete moment-resisting frame buildings exhibiting varying degrees of torsional irregularity and diverse plan shapes is analyzed under different earthquake excitations. The study conducts a total of 3200 linear and nonlinear time history analyses. These analyses are performed across five levels of strength ratios in the buildings, using a suite of 20 far-field ground motions. The torsional floor acceleration amplification factor—defined as the ratio of 5%-damped floor spectral ordinate at the flexible or stiff edge to that at the center of rigidity—is evaluated as a function of the tuning ratio. The relationships between the peak torsional floor acceleration amplification factors and the building's torsional irregularity index are examined for rigid, flexible, and very flexible secondary systems. The torsional floor acceleration amplification factors for rigid and flexible secondary systems depend on building characteristics, namely the extent of torsional irregularity, the strength ratio (level of inelasticity), and the tuning ratio, whereas very flexible secondary systems remain insensitive to them. A strong correlation exists between the torsional floor acceleration amplification factors of rigid and flexible secondary systems and their corresponding building's elastic floor displacement-based torsional irregularity index. Novel equations are developed for predicting torsional floor acceleration amplification factors in buildings with torsional irregularities. When integrated with the latest provisions of ASCE 7, these equations provide accurate estimates of floor acceleration demands, thereby improving seismic design of acceleration-sensitive secondary systems in torsionally irregular buildings.
72.	Transforming RF reflections into respiratory intelligence through radar-ML synergy **A Hari, B Kumbhani, S Darshi, S Agarwal** - IEEE Journal of Radio Frequency Identification, 2026 **Abstract:** Radar-based contactless monitoring of respiratory rate (RR) plays an important role in a person’s life as it provides a new way of patient observation that does not require physical contact, which medical professionals need for monitoring patients in neonatal intensive care units (NICU) because it safeguards their well-being while maintaining their comfort and stopping the spread of diseases. In this paper, we conduct a comprehensive evaluation of various machine learning (ML) models that use continuous wave (CW) radar data to determine noncontact RR measurements. In a previous paper, we showed that the random forest (RF) algorithm can accurately predict RR but is not up to mark for medical purposes. This study systematically investigates different ML algorithms, which include linear regression (LR), support vector regression (SVR), gradient boosting regression (GBR), XGBoost regression (XGBR), and light gradient boosting machine regression (LGBMR) to evaluate their ability to make predictions and their system performance. These algorithms alone do not provide an accurate prediction of RR monitoring, so we introduce a new hybrid algorithm called stacked ensemble regression (SER), which utilizes an SER framework that integrates various base regressors through a meta-learning method to achieve shared benefits, which allow it to capture both vast linear patterns and small nonlinear changes within respiration data. The proposed SER method achieves an accuracy of 92.24%, which surpasses the performance of XGBR, which achieves an accuracy of 89.65%. The proposed framework creates a strong and expandable system that enables monitoring respiratory patterns through both physical and remote methods while developing radar-based respiratory assessment technology for medical use in hospitals and home care environments.
73.	UAV-assisted-IRS-aided-UE: Analysis of ergodic capacity, outage probability, and diversity order N Goel, P Kumar, R Singh, S Jain…**S Darshi** - IEEE Wireless Communications Letters, 2026

	Abstract: Unmanned aerial vehicle (UAV)-assisted transmission provides adaptive and flexible coverage, however, it is constrained by limited transmission range and data rate. Complementing these limitations, intelligent reflecting surface (IRS) assistance emerges as a promising solution. Despite dynamic topology and dynamic environment, existing works are largely based on the ideal or fixed Rician channels, often overlooking the impact of altitude. In light of this, the letter proposes a UAV-assisted-IRS (UA-IRS)–aided communication framework among ground users (GUs) to enhance overall connectivity under practical channel constraints and altitude considerations. Specifically, a comprehensive mathematical framework is developed by modeling the air-to-ground (A2G) link as a height-dependent Rician fading channel. Closed-form expressions for the upper bound on the ergodic capacity are derived, along with an accurate approximation of the outage probability. Furthermore, simplified asymptotic expressions are obtained, and results are provided to validate the theoretical analysis. The study also offers important theoretical insights, including the impact of the IRS order on diversity gain and the influence of height-dependent channel realization on the achievable coding gain.
74.	Vitamin D3 and K2-loaded keratin nanoparticles inhibit breast cancer cell growth via MCM-7 downregulation and ROS induction S Mukherjee, **K Bhavya,** S Dan, **D Pal,** MK Sah - International Journal of Biological Macromolecules, 2026 **Abstract:** The overexpression of the MCM-7 gene, a key player in the minichromosomal maintenance complex critical for DNA replication initiation, is linked to various aggressive cancers. Despite MCM-7's importance in cancer therapy, its amino acid structure has only recently been elucidated, and no clinical trials with small molecular antagonists have been pursued. The present study highlights the anticancer potential of vitamins D2, D3, and K2-loaded keratin nanoparticles, exploring a novel approach to cancer treatment. We found that NPD3 and NPK2 have more anti-proliferative effects than NPD2 through rigorous in-vitro assays utilizing the MCF-7 human breast cancer cell line, known for MCM-7 overexpression. Mechanistically, NPD3 exerts its anticancer effect by downregulating MCM-7 protein expression, while NPK2 induces intracellular ROS generation. The study involves a nanocarrier system derived from human hair keratin, enhancing the bioavailability and efficacy of these vitamins. These nanocarriers not only improve the anti-proliferative effects of the vitamins but also demonstrated exceptional biocompatibility and controlled drug release in response to pH changes. These findings propose a novel, commercially viable delivery system for water-insoluble vitamins, offering a promising therapeutic avenue against cancers with MCM-7 overexpression. 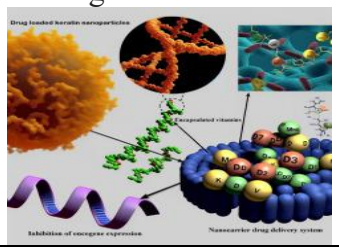

Disclaimer: This publication digest may not contain all the papers published. Library has compiled the publication data as per the alerts received from Scopus and Google Scholar for the affiliation “Indian Institute of Technology Ropar” for the month of May, 2026. The author(s) are requested to share their missing paper(s) details if any, for the inclusion in the next publication digest.